ISSN: Applied
Int. J. Eng. & Innovations, 1.1 (2019) pp.1-26

Research Article

LOSS OF HEAD DUE TO NON-UNIFORM FLOW THROUGH POROUS MEDIA

Dr. N. BhanuPrakasham Reddy[1], Dr. S. Krishnaiah[2], Dr. M. Ramakrishna Reddy[3]

[1]Assistant Executive Engineer, Water Resources Department, Design Division No.1, O/o NTRTGP, Tirupati - 517501, Chittoor District, Andhra Pradesh State, India, e-mail : nbpreddy@gmail.com or nbpreddy@rediffmail.com, Mobile Number: +91 9989283051.

[2]Professor of Civil Engineering, J.N.T.U.A. College of Engineering, Anantapur - 515002, Andhra Pradesh State, India, e-mail : sankranthikrishnaiah@gmail.com, Fax: 08554 272098, 08554 272210 (R), Mobile Number: +91 9849772885.

[3]Professor of Earth Science, Yogivemana University, Kadapa – 516004, Y.S.R. District, Andhra Pradesh State, India, e-mail: reddy.mrk@rediffmail.com, Fax : 08562 225419, 08562 225443 (R), Mobile Number: +91 9441325055.

Abstract: Study of seepage flow through soil strata of convergent confined aquifer is of complex nature. An attempt has been made to analyse the resistance of fluid flow through convergent duct with dimensions along transverse direction varying from 1000 mm at top and 200 mm at bottom and the height of the duct along longitudinal direction is 1050 mm and width of duct between two parallel confining surfaces is 200 mm filled with porous media of size 14.50 mm crushed rocks for better understanding purpose for certain extent. The total energy loss per unit weight of flowing fluid through boundary of the convergent duct and along the centre of the convergent duct for different bed slopes varying from 60^0 to 90^0 are analysed. The variation of Darcy parameter, a_c, and non-Darcy parameter, b_c, which are influenced by the properties of the fluid and porous media, are determined from a plot of i/V versus V along the longitudinal direction of converging duct and along the transfers direction of converging duct are studied to explore the indescribable complex nature of resistance flow through porous media. It is also investigated how the volume flux of fluid is affected when it flows through convergent duct when the media is being packed with porous media with varying bed slopes from 60^0 to 90^0.

Keywords: Non-Uniform Flow; Darcy Parameter; Non-Darcy Parameter, Porous media; Bed Slopes; Convergent Duct

List of nomenclature and abbreviations:

The following symbols and abbreviations are used

a = linear parameter or Darcy parameter;

a_c = linear parameter or Darcy parameter with convergence effect;

a_p = linear parameter or Darcy parameter for parallel flow;

B_1, B_2 …etc., = width of duct at piezometric tapping points 1, 2…etc.;

b = non- linear parameter or non-Darcy parameter;

b_c = non- linear parameter or non-Darcy parameter with convergence effect;

b_p = non- linear parameter or non-Darcy parameter for parallel flow;

C_W = media constant;

F_k= friction factor using $\sqrt{k}$ as the characteristic length;

F_K^2 = square of Froude Number using $\sqrt{k}$ as the characteristic length;

G = acceleration due to gravity;

h_f=head loss;

I = hydraulic gradient;

K_A and K_B = convergence factors;

k = intrinisic permeability;

L = length of travel;

N =porosity;

p_1, p_2…etc.=piezometric head at piezometric tappings 1,2,…etc.,;

Q = rate of flow;

R = radius from the centre of convergence;

R_1,R_2,..etc.= radial distance of piezometric tappings 1,2,….etc.,;

R_k = Reynolds number using $\sqrt{k}$ as the characteristic length;

V = macroscopic velocity or seepage velocity;

V_1 = seepage velocity at section 1;

W = width of flow between two parallel confining surfaces;

θ = angle of convergence in radians;

μ = dynamic viscosity of fluid;

ν = kinematic viscosity of fluid;
ρ = density of the fluid; and
φ = tilting angle or angle of inclination of duct;
CSL Convergent stream line
CSL-1 Convergent stream line - 1
CSL-2 Convergent stream line - 2
CSL-3 Convergent stream line - 3
DPCE or LPCE: Darcy parameter or linear parameter with convergent effect;
FFSRIP: Friction factor using $\sqrt{k}$ as the characteristic length;
NDPCE or NLPCE: Non-Darcy parameter or non-linear parameter with convergent effect;
RNSRIP: Reynolds number using $\sqrt{k}$ as the characteristic length;
SFNSRIP: Square of Froude Number using $\sqrt{k}$ as the characteristic length;
SRIP: Square root of intrinsic permeability;

I Introduction

The study of seepage flow patterns in converging cross-section with porous media of varying angle of inclination is one of the most worthwhile and rewarding applications especially in hydrology, which relates to water movement in earth and sand or rock structures such as Earthen dams or Rock fill dams, flow to wells from water bearing formations, intrusion of sea water in coastal areas, filter beds for purification of drinking water and sewage etc.,

Forchheimer (Scheidegger 1963) conducted experiments on a sand-box model and proposed an equation in a quadratic form as,

$$I = aV + bV^2 \quad \ldots (1)$$

for the non-linear regime of flow, in which a and b are the coefficients determined by the properties of the fluid and porous media, and are known as Darcy or linear parameter and non-Darcy or non-linear parameter.

A glance at Forchheimer 's equation relating hydraulic gradient and seepage velocity, written in the modified form as

$$I/V = bV + a \quad \ldots (2)$$

The values of a and b are obtained from a plot of I/V vs. V, which is a straight line.

Ward (1964) developed an equation dimensionally for both laminar and turbulent flows in porous medium as

$$I = \frac{\mu V}{\rho g k} + \frac{C_W V^2}{g\sqrt{k}} \quad \ldots (3)$$

in which I is hydraulic gradient and g is acceleration due to gravity. Comparing the Forchheimer's Eq. (1) with Eq. (3), Ward obtained an expressions for a and b as

$$a = \frac{\mu}{\rho g k} \quad \ldots (4)$$

and

$$b = \frac{C_W}{g\sqrt{k}} \quad \ldots (5)$$

where k = intrinsic permeability; ρ = density of the fluid; μ = dynamic viscosity; and C_W = media constant.

Ward obtained the relationship between the FFSRIP, F_k and RNSRIP, R_k by defining FFSRIP, F_k as $\frac{Ig\sqrt{k}}{V^2}$ and RNSRIP, R_k as $\frac{V\sqrt{k}}{\nu}$ and using SRIP, $\sqrt{k}$ as the characteristic length as

$$F_k = \frac{1}{R_k} + C_W \quad \ldots (6)$$

Bhanu Prakasham Reddy (2006) developed an expression incorporating the effect of convergence on the LPCE or DPCE, a_c, and NLPCE or NDPCE, b_c, when flow occurs through porous media with converging boundaries as

$$I = a_C V_1 + b_C V_1^2 \quad \ldots (7)$$

Where V_1 = seepage velocity at section 1;
a_c and b_c = Coefficients for converging flow given by

$a_c = K_A a_p$ … (8)

and $b_c = K_B b_p$ … (9)

where K_A and K_B are constants represents the effect of convergence on the coefficients a_p and b_p and may be termed as "Convergence factors"

$$K_A = \left[\frac{LOG\left(\frac{B_1}{B_2}\right)}{\left(1-\frac{B_2}{B_1}\right)}\right] \quad \ldots(10)$$

and $$K_B = \left[\frac{B_1}{B_2}\right] \quad \ldots(11)$$

where B_1 and B_2 are the width of duct at piezometric tapping points 1 and 2 at radii R_1 and R_2 respectively.

Eq. (8) and Eq.(9) together with Eq.(10) and Eq.(11) shows that the effect of converging boundaries for a given discharge Q depends only on the width of the duct at piezometric tapping points p_1 and p_2.

Bhanu Prakasham Reddy (2006) investigated the influence of convergent factors on the resistance law relating FFSRIP, F_k and RNSRIP, R_k using SRIP, $\sqrt{k}$ as characteristic length was examined.

Reddy *et al.,* (2014) investigated that the variation of FFSRIP, F_k with RNSRIP, R_k increases with increase of convergent angle for the same R_1/R_2 ratio and also studied the variation of FFSRIP, F_k and RNSRIP, R_k for different C_W values for different convergent angles (θ) and for different ratios of radii are compared with the experimental data and observed lie on the theoretical curve.

Reddy *et al.,* (2014a) studied the relationship between Hydraulic Gradient (I) and SFNSRIP, F_K^2 for flow through porous media with converging boundaries, using SRIP, $\sqrt{k}$ as characteristic length for different convergent angles and it has been concluded that the variation of hydraulic gradient (I) with SFNSRIP, F_K^2 is increased for small convergent angle (θ) for any R_1/R_2 ratios when compared to the large convergent angle (θ). Also shown pictorially the relation between LPCE or DPCE, a_c, and NLPCE or NDPCE, b_c, in terms of Media Constant (C_W) and concluded that as convergent angle (θ) is increased, both LPCE or DPCE, a_c, and NLPCE or NDPCE, b_c, increases, and also the values of a and b increases with the increase in convergent angle.

In the case of parallel flow or uniform flow through porous media, since cross sectional area of flow is constant along the length of travel of flow, the velocity is same at any point and the hydraulic gradient (I) is same for a given discharge and size of the media. Therefore, linear parameter, a_p and non-linear parameter, b_p values are constant for a discharge and size of the media. But in the case of Convergent flow or Non - Uniform flow through porous media, since cross-sectional area of flow changes along the length of travel of flow, the velocity changes from point to point, hence the hydraulic gradient (I) also varies from point to point for a given discharge and size of the media. Therefore, LPCE or DPCE, a_c, and NLPCE or NDPCE, b_c, values are varied along the length of travel of flow.

A glance at the literature reported so far that, most of the investigators have been carried out research on flow through porous media with parallel boundaries. A little work has been reported in the literature on the studies describing behavior of flow through porous media with convergent boundaries. It is opined that this investigation may clarify some of the concepts concerning the steady non uniform flow of fluid through varying porous media when the media is being packed between tilting angled convergent boundaries.

II Experimental apparatus

The experimental flow studies were performed in converging tilting angle duct having a converging portion of 1050 mm high and of width varying from 1000 mm at top and 200 mm at bottom. The angle of convergence is 41.71^0 (0.73 radians) and width of duct between two parallel confining surfaces is 200 mm. The converging sides and rear portion of the duct are made of 6 mm M.S. sheet and the front face of the Duct is made of 12.5 mm flexi glass window for viewing the flow in the media. Piezometric tapping points are provided at 50 mm spacing and connected to a manometer board facilitated measurement of piezometric heads along the duct.

The entire set up is rest on the bearings and is housed in a strong M.S. supports. The tilting arrangements of the duct are made by means of teethed wheels and chain with lock on the left side of the M.S. support. The tilting angle index is fixed on the right side of the M.S. support to read tilting angle or bed slope of the duct from 90^0 to 30^0. A schematic diagram of the experimental arrangement is shown in Fig.1.

A fixed flow was allowed in the system to maintain a constant head in the header tank. Head loss measured between any two piezometric head points located at radii R_1 and R_2 and Hydraulic gradient (I) is obtained from the equation

$$I = \frac{h_f}{L} = \left(\frac{p_1 - p_2}{R_1 - R_2}\right) \qquad \ldots(12)$$

Where Head loss (h_f) = Difference in piezometric heads between any two points located at radii R_1 and $R_2$and L = Length of travel of flow between any two points located at radii R_1 and R_2.

The flow rate (Q) through the media was measured by the volumetric method by using a graduated measuring tank of size 0.6 m X 0.6 m X 0.6 m is used and the velocity of flow V at any radius R from the centre of convergence is given by

$$V = \frac{Q}{R\theta WN} \qquad \ldots (13)$$

Where Q is flow rate in cm^3/sec, θ is angle of convergence in radians, W is width of flow between two parallel confining surfaces of the converging duct and N is the porosity. Experiments were conducted at different rate of flow through the media for each tilting angle or bed slope of the duct and the head losses in the duct were measured.

III Determination of porosity

The porosity is determined by filling the duct with the medium under gravity up to the top without any compaction. A liquid of measured quantity is then poured between bottom piezometer up to the top of the piezometer. The volume of the duct enclosed between these two piezometers is computed from the geometry of the duct. The porosity is computed by the ratio of volume of voids to the volume of the duct.

In the present investigation, the porosity is measured between different Piezometric tappings depends on length of travel of flow as shown in Fig.2 i.e., between Piezometric tapping 1 and 2 (R_1/R_2), between Piezometric tapping 1 and 3 (R_1/R_3), and so on up to between Piezometric tapping 1 and 18 (R_1/R_{18}). The effect of variation of porosity is also considered while computing seepage velocity (V) using Eq. (13) for different length of travel of flow and it is same for all other tilting angles.

IV Results and Discussions

Variation of Piezometric Head (H) with Location of Piezometric Points:

The variation of piezometric head (H) with Location of piezometric points for different rate of flows (Q), tilting angles (φ) and size of the media are depicted in Fig.3 to Fig.6. It is observed from these figures that the piezometric head (H) varies along the lateral direction along CSL with respect to the location of piezometric Points as shown in Fig. 2.

It is noticed that the piezometric head (H) decreases from CSL-1 to CSL-3 for each rate of flows (Q), tilting angles (φ) and size of the media. It is also observed that piezometric Head (H) decreases with increase of rate of flows (Q) for each tilting angles (φ) and size of the media and observed that the piezometric head (H) increases with increase of the distance of the Location of piezometric points from the convergent portion. i.e., piezometric head (H) decreases along the direction of flow as the velocity of flow increases due to decreases of area of flow.

Variation of i/V with V for different Tilting Angles(φ) and Ratio of Widths (B_1/B_2):

The variation of i/V with V for different tilting angles (φ), ratio of widths (B_1/B_2) and size of media are shown in Fig.7 to Fig.9.

Fig.7 to Fig.9 shows the variation of i/V vs. V for different tilting angles (φ) and ratio of widths (B_1/B_2) and size of media for 14.50 mm crushed rock.

It is seen from these graphs that i/V, which is a measure of total energy loss in the medium, increases as seepage velocity is increased for any B_1/B_2 ratio and i/V decreases as the B_1/B_2 ratio decreases for any size of the media and for any tilting angle (φ). It is also observed that as the size of the medium increases i/V decreases with V for any B_1/B_2 ratio and tilting angle (φ) i.e., as the size of the medium increases, the porosity of the medium increases and therefore the total energy loss decreases.

The variation of i/V with V for different CSL and tilting angles (φ) and for different B_1/B_2 ratios are depicted in Fig.10 to Fig.13. It is observed that i/V increases as the seepage velocity (V) increases for any tilting angle (φ) andB_1/B_2 ratios and for any size of the media. It is noticed that i/V increases with increase of tilting angle (φ) for any B_1/B_2 ratios and for any size of the media.

Fig.10 to Fig.13 illustrates the variation of i/V with V along lateral direction and along the direction of flow from CSL-1 To CSL-3 for different B_1/B_2 ratios and tilting angle (φ) for 14.50 mm crushed rocks. It is seen that i/V increases with increases of V for different CSL for different B_1/B_2 ratios and tilting angles (φ) and also observed from these figures that i/V, which is a measure of total energy loss in the medium, increases near the convergent boundary i.e., CSL-1 and decreases towards central CSL-3.

Evaluation of a_c and b_c for different Bed Slopes (φ):

Fig.3 to Fig.9 shows the plots of I/V versus V for the experimental data of the present study for 14.50 mm crushed rock using water as the fluid. When a plot is prepared between I/V versus V using Eq.2, the slope of the line indicates the NLPCE or NDPCE, b_c, while the LPCE or DPCE, a_c, is equal to the intercept of the ordinate of the plot. The LPCE or DPCE, a_c, and NLPCE or NDPCE, b_c, can be computed by selecting an approach section arbitrarily at radius R_1 and an exit section at radius R_2. Based on the flow rates and the piezomeric heads at these two points, the seepage velocity and the hydraulic gradient are computed.

The values of the coefficients a_c and b_c for this R_1/R_2 ratio are then obtained from a plot of I/V versus V, which is a straight line, where V is velocity at section at R_1 equal to flow rate Q / flow area A_1 at approach section. Linear equation fitted to these lines by the method of least squares yields the values of a_c and b_c for that particular R_1/R_2 ratio.

This procedure is repeated for different ratios of R_1/R_2 to get different values of a_c and b_c with the same media. Similarly, different values of a_c and b_c are computed for different tilting angles or bed slopes (φ).

Variation of LPCE or DPCE, a_c, and NLPCE or NDPCE, b_c, with Ratio of Width (B_1/B_2) for Different Convergent Stream Lines (CSL) and Tilting Angles (φ)

Fig. 14 to Fig. 15 illustrates the variation of LPCE or DPCE, a_c, and NLPCE or NDPCE, b_c, with ratio of width (B_1/B_2) along lateral direction and along the direction of flow from CSL-1 to CSL-3 for different bed slopes (φ) for 14.50 mm crushed rocks.

It is observed from these figures that LPCE or DPCE, a_c, and NLPCE or NDPCE, b_c, decreases with decrease of ratio of width (B_1/B_2) for different CSL and tilting angles (φ) and the same trend is observed for all CSL and tilting angles (φ).

Fig. 14 to Fig. 15 depicts that both LPCE or DPCE, a_c, and NLPCE or NDPCE, b_c, decreases along the lateral direction from CSL-1 to CSL-3 and increases along the direction of flow for all CSL and tilting angles (φ).

V Conclusions

The effect of tilting angle and varying porosity on non- uniform flow through porous media has been analyzed in a converging duct. The experimental results are emphasized that tilting angle has a significant effect on non-uniform fluid flow through porous media when the media were confined within a convergent configuration and is noticed that the velocity of flow increases with increase of tilting angle (φ). It is also noticed that I/V, which is a measure of total energy loss in the medium decrease with increase of tilting angles from 60^0 to 90^0 and is decreased with decrease of width ratios for any tilting angle or bed slope (φ).

The non-uniform fluid flow through converging boundary, the parameters a_c and b_c, represents the property of fluid and porosity, vary along the direction of flow as the velocity of flow increases and the porosity decreases along the direction flow and observed that the values of a_c and b_c increases with the decrease of tilting angles (φ) from 90^0 to $60^0$and It is seen from the results that both a_c and b_c increases linearly with the increase of width ratio's for any tilting angle (φ). It is inferred from the results and discussion that the width ratio increases denotes that the length of travel of fluid increases resulting in the increase in resistance flow.

Acknowledgements

The authors wish to thank the Ministry of Science & Technology, Department of Science and Technology, New Delhi, authorities for the financial support (Grant No: SR/FTP/ETA -22/2005) rendered by them for carrying out the study. The authors also wish to acknowledge the encouragement given by the Management and Director of N.B.K.R. Institute of Science & Technology, Vidyanagar, Nellore District during study.

References

[1] Bhanu Prakasham Reddy, N., Krishnaiah, S., and Rama Krishna Reddy, M., Convergent Angle Effect on Non - Uniform Flow Through Porous Media, Journal of Information., Knowledge and Research in Civil Engineering, Vol. 3(1), pp. 152- 159, 2014.

[2] Bhanu Prakasham Reddy, N., Krishnaiah, S., and Rama Krishna Reddy, M., Effect of Convergent Angle on Non-Uniform Flow through Porous Media, ISH Journal of Hydraulic Engineering., Vol.21(1), pp. 53-64, 2014.

[3] Bhanu Prakasham Reddy, N., and Rama Krishna Reddy, M., Energy loss in the flowing fluid through porous media with convergent boundaries, Journal of Indian Water Resources Society., vol.30(3), pp. 30-36, 2010.

[4] Bhanu Prakasham Reddy, N., and Rama Krishna Reddy, M., Efficiency of steady non-uniform flow through homogeneous porous media, Journal of Hydraulic Engineering., vol.13(2), pp. 53-65, 2007.

[5] Forchheimer, P., Wasserbewegungdurch Boden, Z. Ver.Deutsch. Ing., 45, pp. 1782-1788, 1901.

[6] Ward, J.C., Turbulent flow in porous media, J. Hydr.Div., ASCE, vol. 90(5), pp.1-12, 1964.

Source of support: Nil; **Conflict of interest:** Nil.

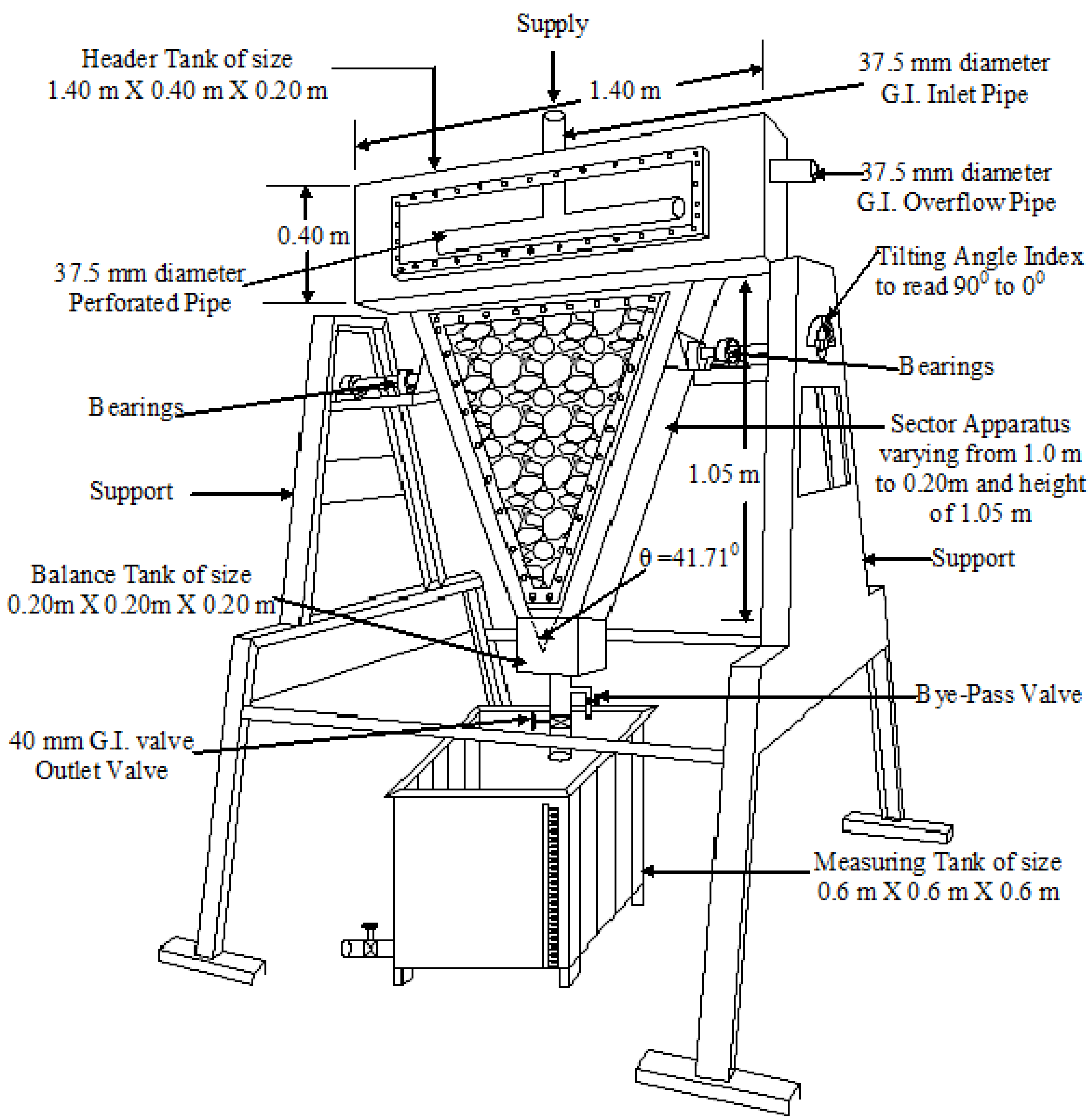

Fig.1. Schematic of Convergent Flow Duct

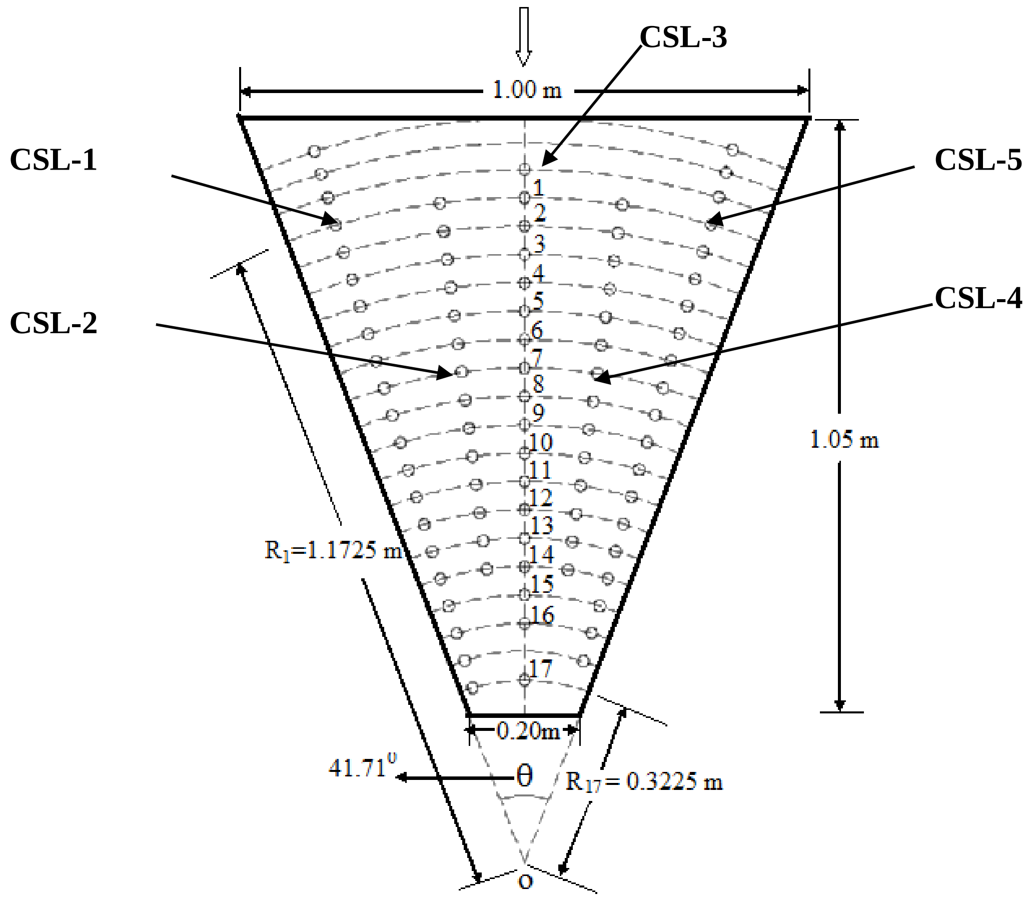

Fig.2. Line diagram of Converging Duct

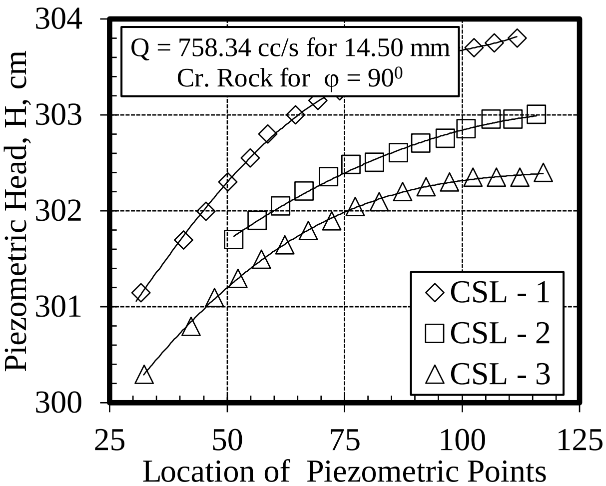

Fig.3.1 H vs Location of Piezometric Points

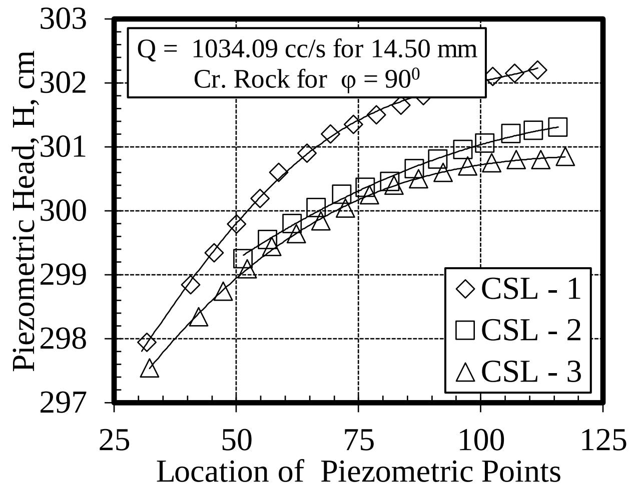

Fig.3.2 H vs Location of Piezometric Points

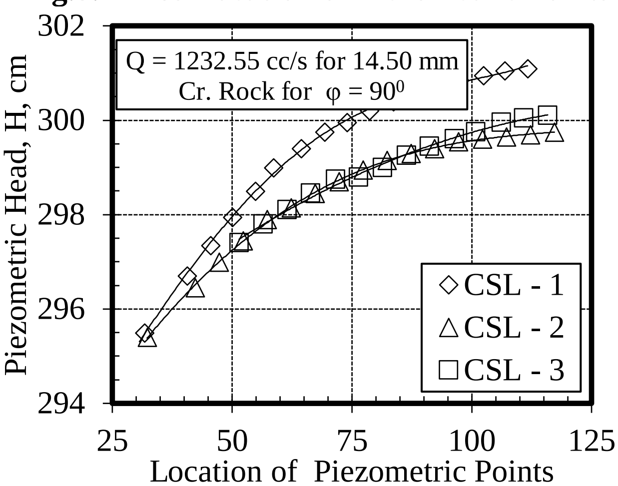

Fig.3.3 H vs Location of Piezometric Points

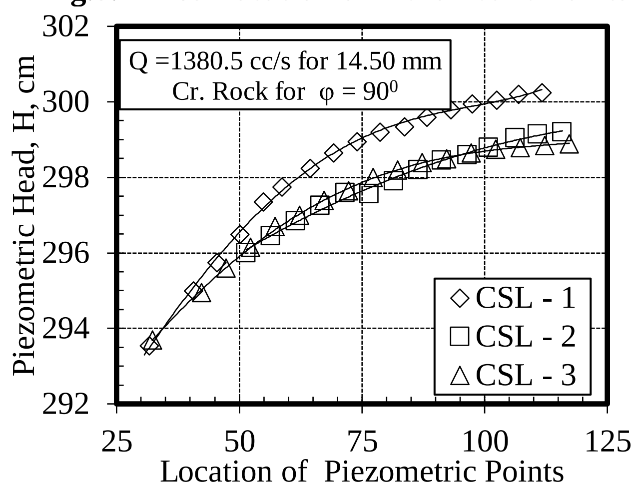

Fig.3.4 H vs Location of Piezometric Points

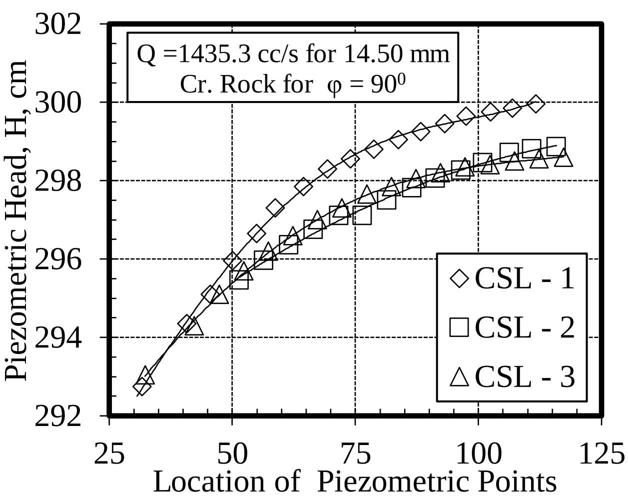

Fig.3.5 H vs Location of Piezometric Points

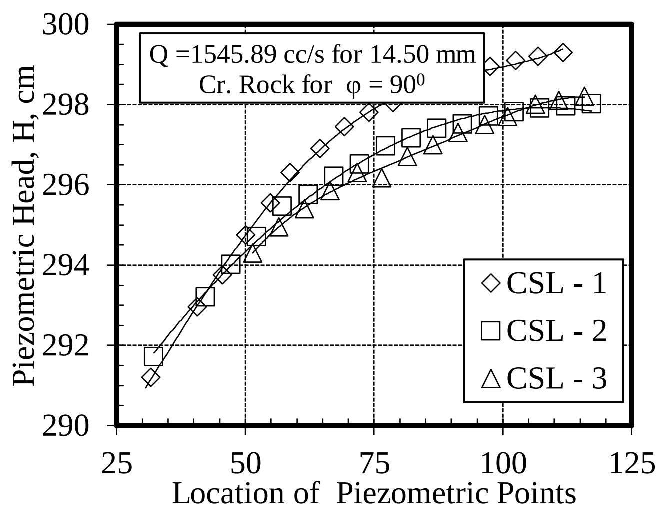

Fig.3.6 H vs Location of Piezometric Points

Fig.3. H vs Location of Piezometric Points for Different Q for 14.50 mm Cr. Rock for $\varphi = 90^0$

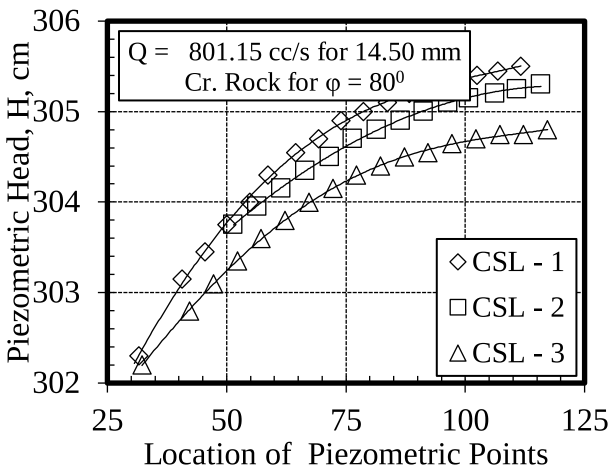

Fig.4.1 H vs Location of Piezometric Points

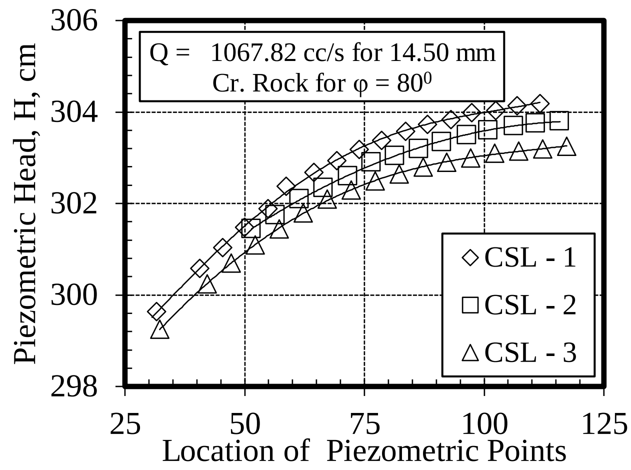

Fig.4.2 H vs Location of Piezometric Points

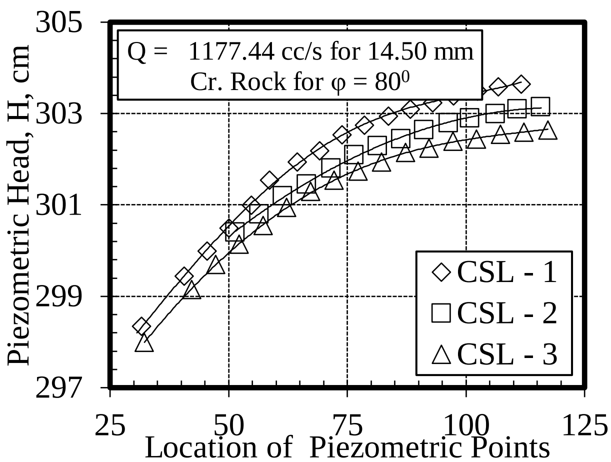

Fig.4.3 H vs Location of Piezometric Points

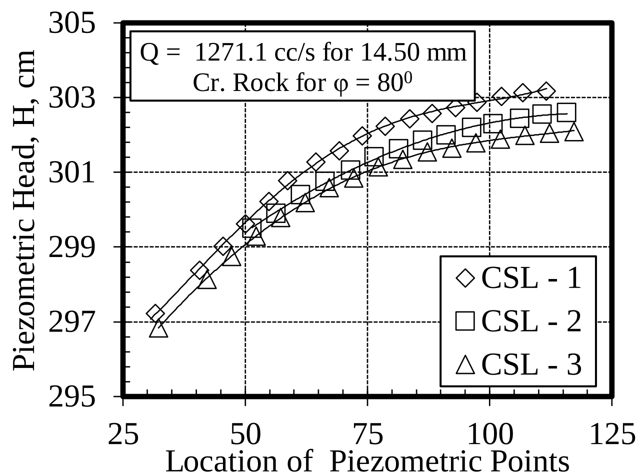

Fig.4.4 H vs Location of Piezometric Points

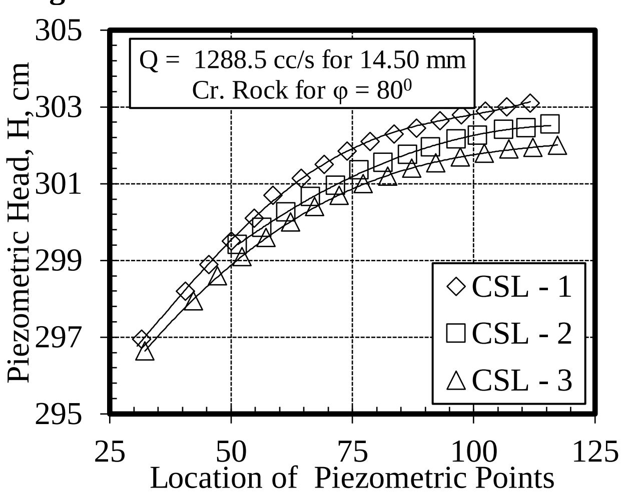

Fig.4.5 H vs Location of Piezometric Points

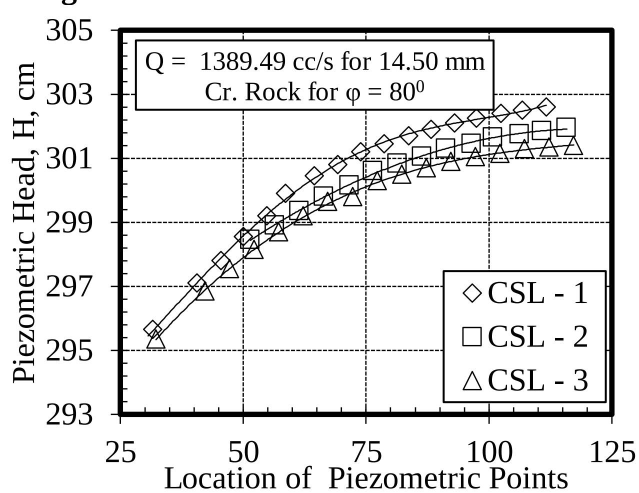

Fig.4.6 H vs Location of Piezometric Points

Fig.4. H vs Location of Piezometric Points for Different Q for 14.50 mm Cr. Rock for $\varphi = 80^0$

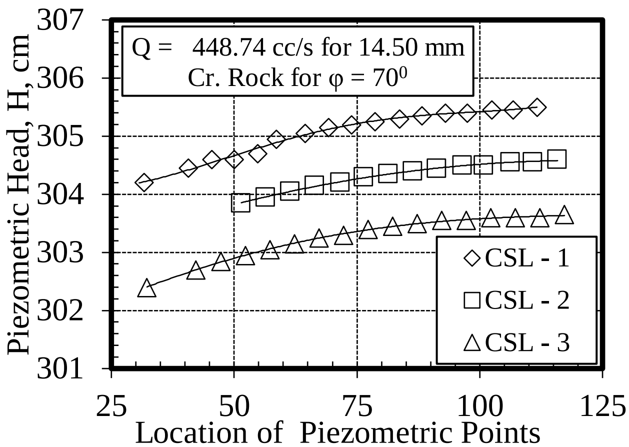

Fig.5.1 H vs Location of Piezometric Points

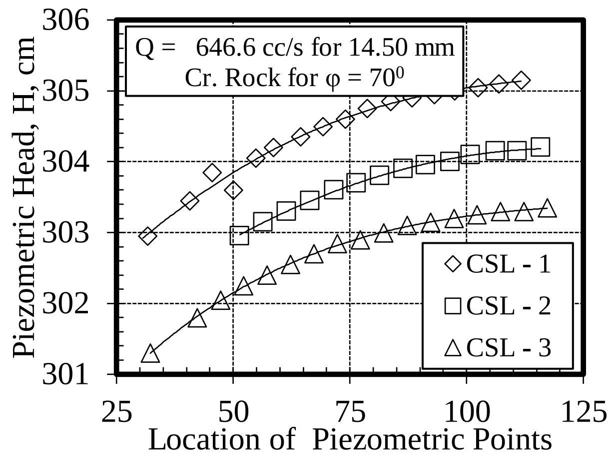

Fig.5.2 H vs Location of Piezometric Points

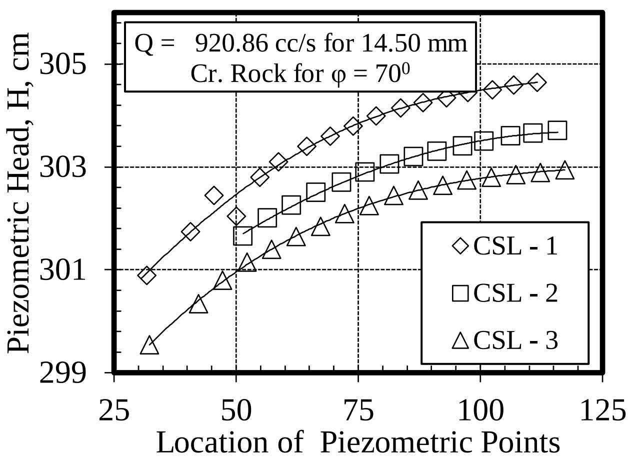

Fig.5.3 H vs Location of Piezometric Points

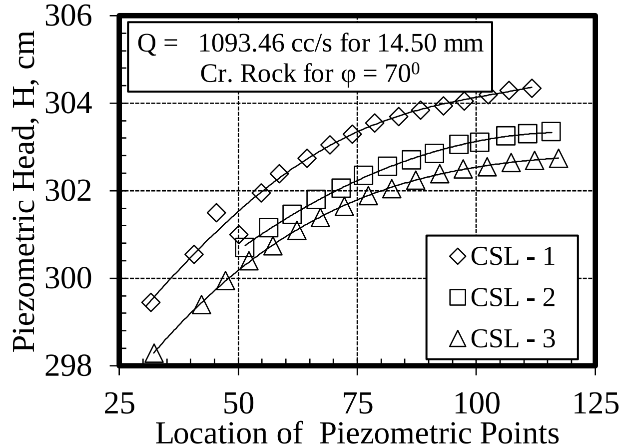

Fig.5.4 H vs Location of Piezometric Points

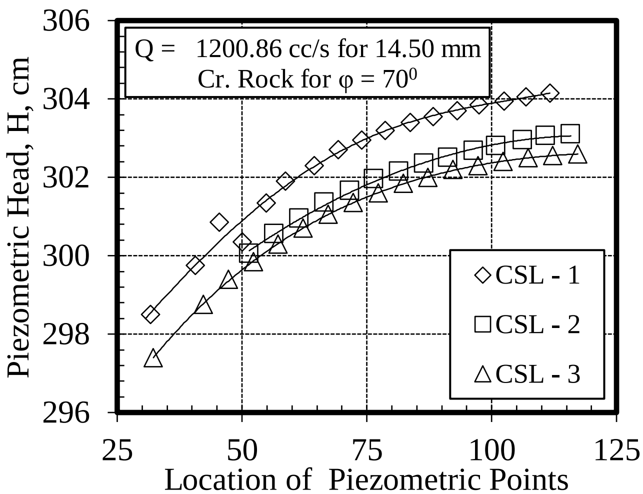

Fig.5.5 H vs Location of Piezometric Points

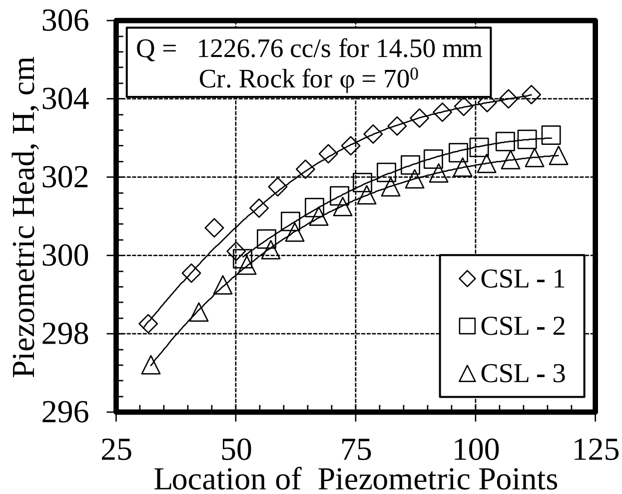

Fig.5.6 H vs Location of Piezometric Points

Fig.5. H vs Location of Piezometric Points for Different Q for 14.50 mm Cr. Rock for $\varphi = 70^0$

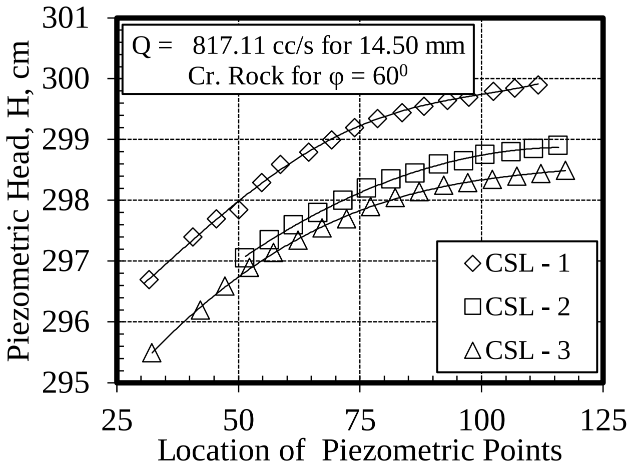

Fig.6.1 H vs Location of Piezometric Points

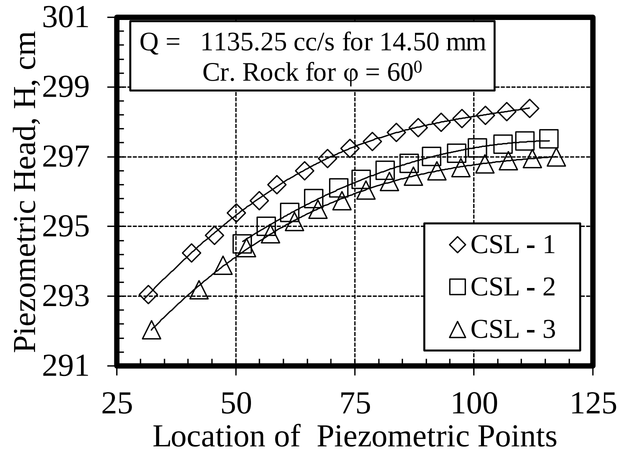

Fig.6.2 H vs Location of Piezometric Points

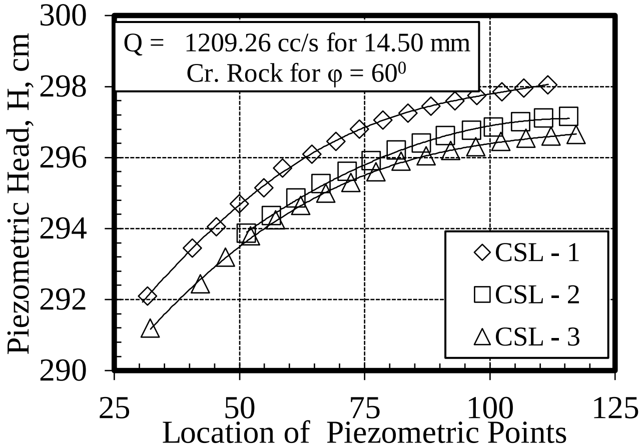

Fig.6.3 H vs Location of Piezometric Points

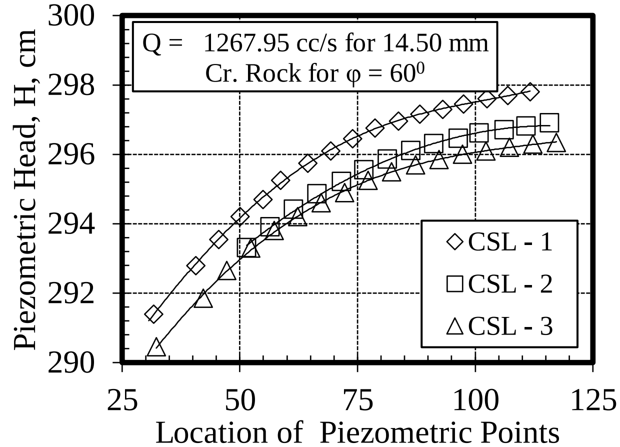

Fig.6.4 H vs Location of Piezometric Points

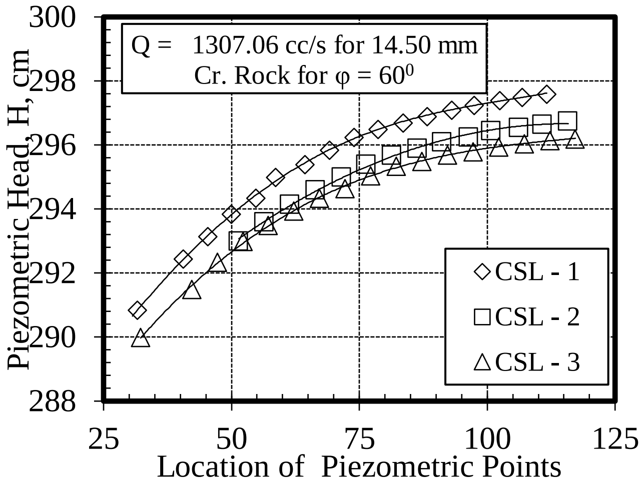

Fig.6.5 H vs Location of Piezometric Points

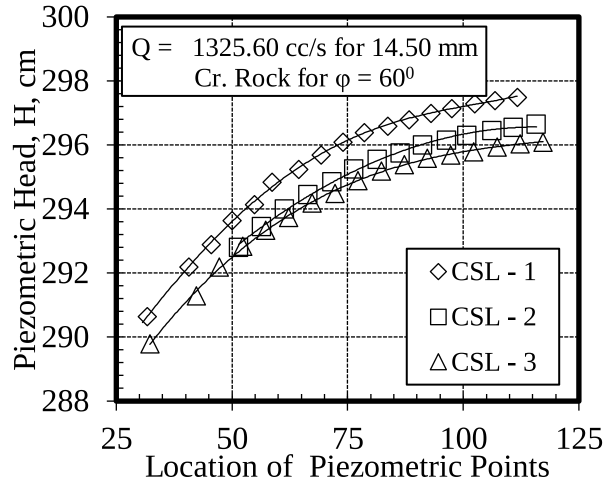

Fig.6.6 H vs Location of Piezometric Points

Fig.6 H vs Location of Piezometric Points for Different Q for 14.50 mm Cr. Rock for φ = 60^0

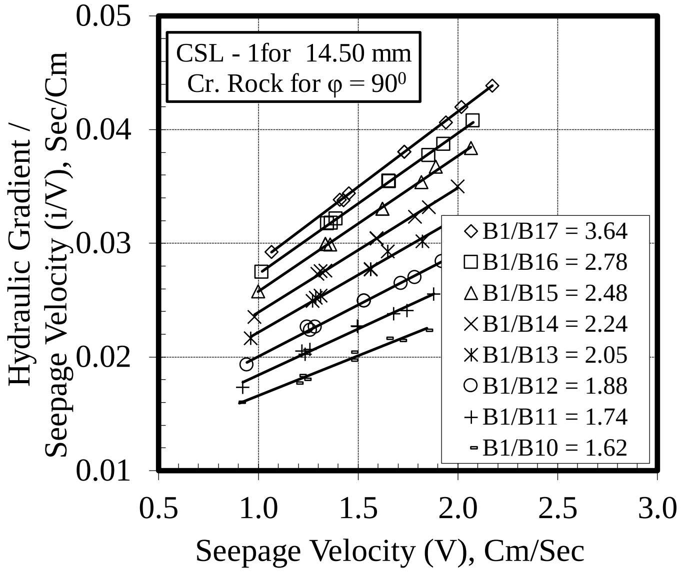

CSL - 1for 14.50 mm
Cr. Rock for φ = 90⁰
Hydraulic Gradient / Seepage Velocity (i/V), Sec/Cm
Seepage Velocity (V), Cm/Sec
B1/B17 = 3.64
B1/B16 = 2.78
B1/B15 = 2.48
B1/B14 = 2.24
B1/B13 = 2.05
B1/B12 = 1.88
B1/B11 = 1.74
B1/B10 = 1.62
0.05
0.04
0.03
0.02
0.01
0.5
1.0
1.5
2.0
2.5
3.0

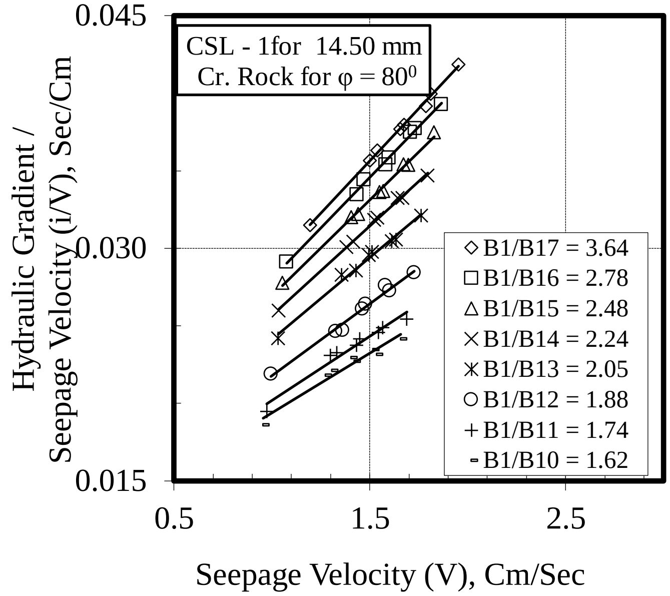

CSL - 1for 14.50 mm
Cr. Rock for φ = 80⁰
Hydraulic Gradient / Seepage Velocity (i/V), Sec/Cm
Seepage Velocity (V), Cm/Sec
B1/B17 = 3.64
B1/B16 = 2.78
B1/B15 = 2.48
B1/B14 = 2.24
B1/B13 = 2.05
B1/B12 = 1.88
B1/B11 = 1.74
B1/B10 = 1.62
0.045
0.030
0.015
0.5
1.5
2.5

Fig.7.1 i/V vs V for φ = 90⁰ for 14.50 mm Crushed Rock

Fig.7.2 i/V vs V for φ = 80⁰ for 14.50 mm Crushed Rock

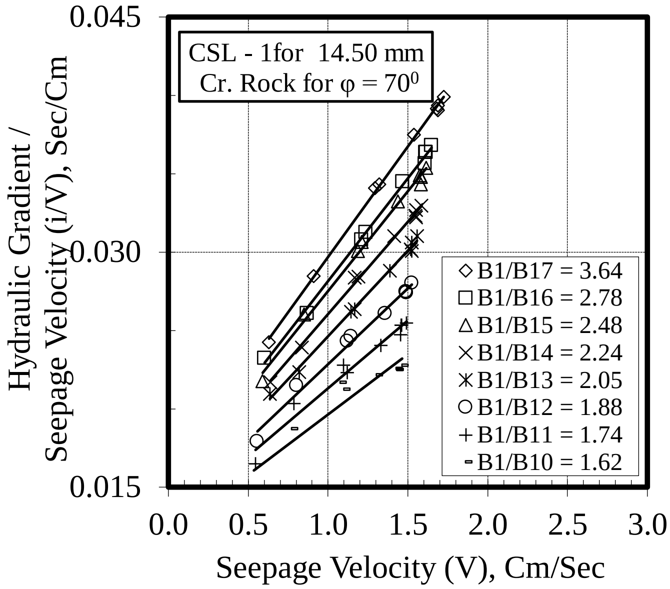

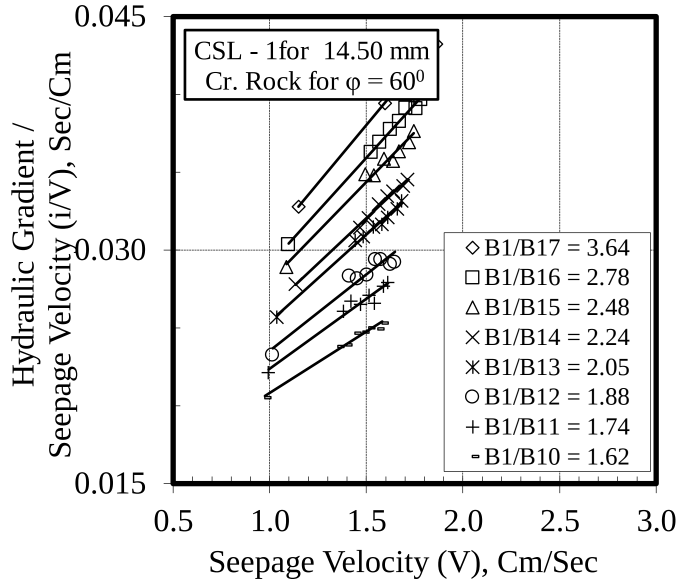

Fig.7.3 i/V vs V for φ = 70⁰ for 14.50 mm Crushed Rock

Fig.7.4 i/V vs V for φ = 60⁰ for 14.50 mm Crushed Rock

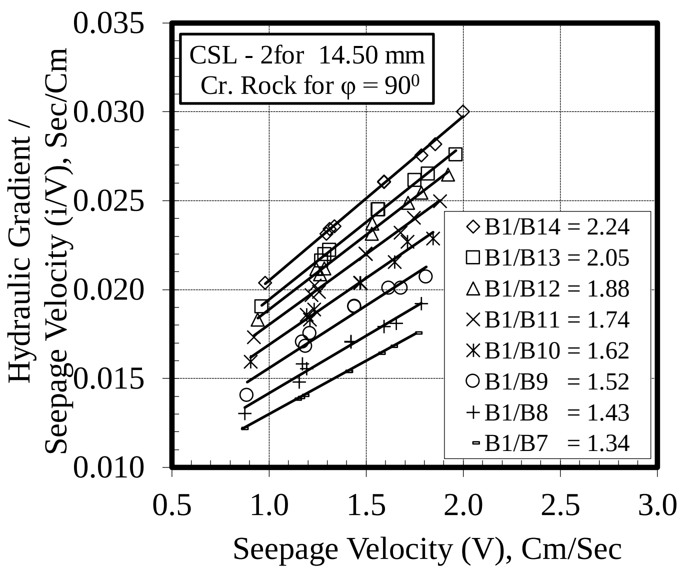

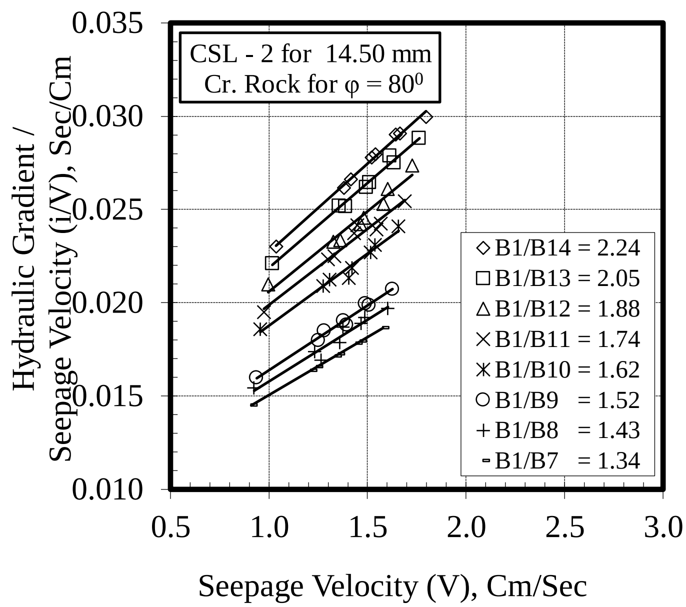

Fig.7 i/V vs V for different B_1/B_2 ratios and Tilting Angles(φ) for CSL -1for 14.50 mm Cr. Rock

Fig.8.1 i/V vs V for $\varphi = 90^0$ for 14.50 mm Crushed Rock

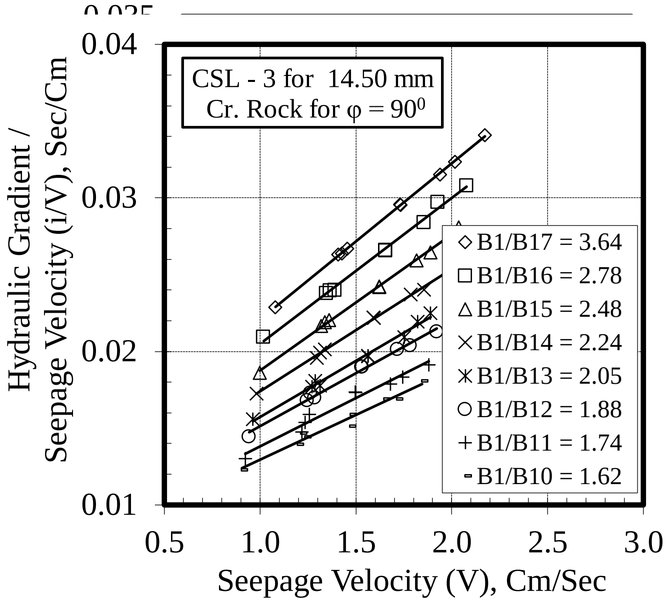

Fig.8.2 i/V vs V for $\varphi = 80^0$ for 14.50 mm Crushed Rock

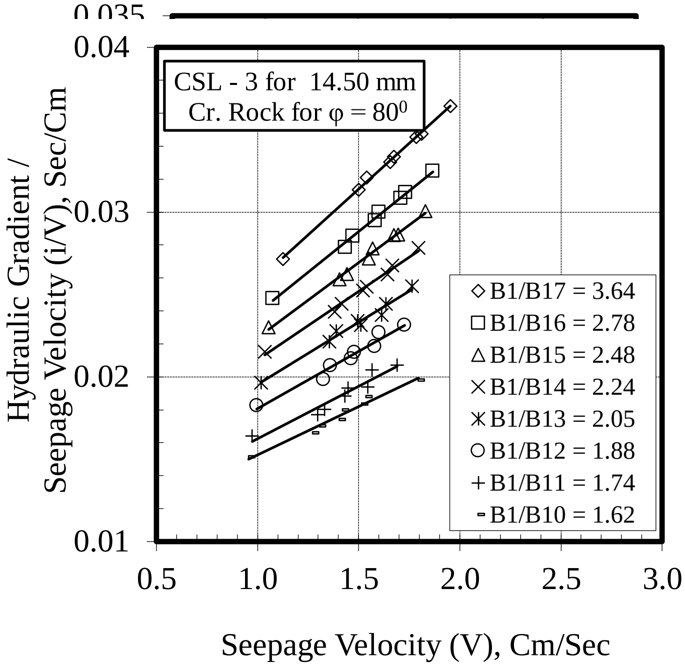

Fig.8.3 i/V vs V for $\varphi = 70^0$ for 14.50 mm Crushed Rock

Fig.9.1 i/V vs V for $\varphi = 90^0$ for 14.50 mm Crushed Rock

Fig.8 i/V vs V for different B_1/B_2 ratios and Tilting Angles(φ) for CSL - 2 for 14.50 mm Cr. Rock

Fig.9.2 i/V vs V for $\varphi = 80^0$ for 14.50 mm Crushed Rock

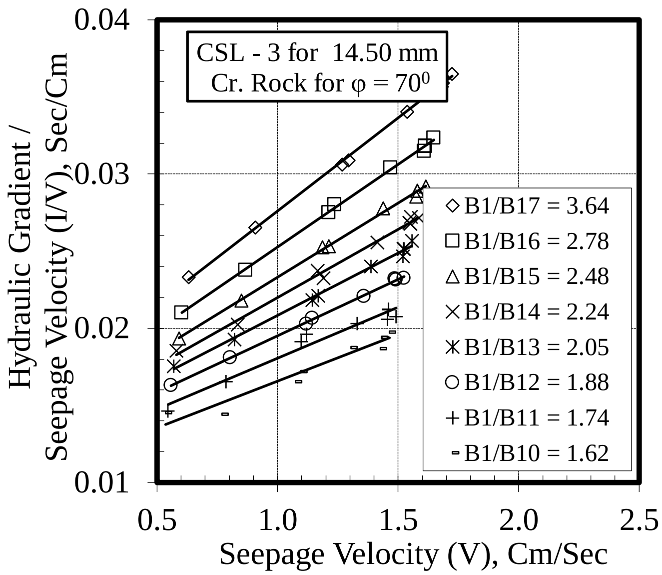

Fig.9.3 i/V vs V for $\varphi = 70^0$ for 14.50 mm Crushed Rock

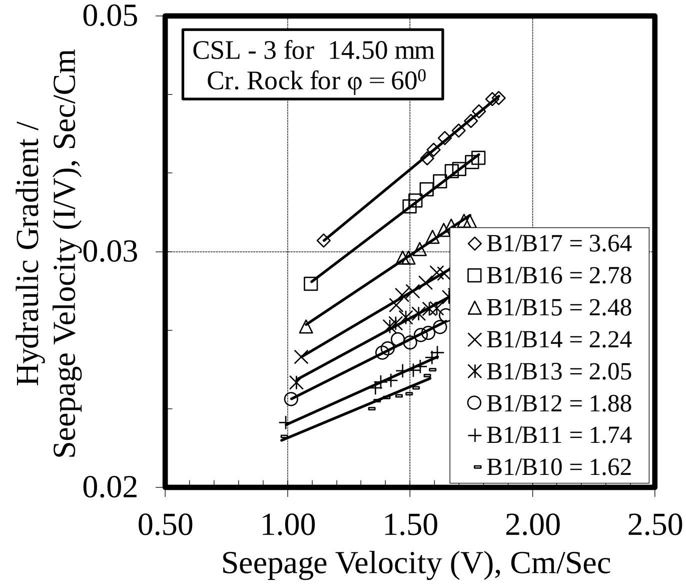

Fig.9.4 i/V vs V for $\varphi = 60^0$ for 14.50 mm Crushed Rock

Fig.9 i/V vs V for different B_1/B_2 ratios and Tilting Angles(φ) for CSL– 3 for 14.50 mm Crushed Rock

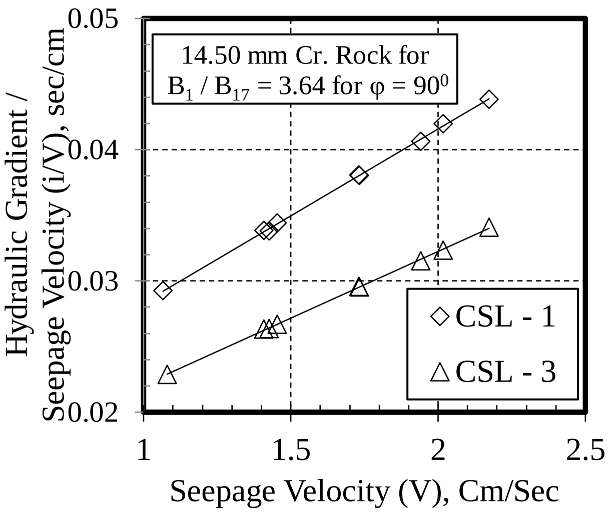

Fig.10.1 i/V vs V for $B_1/B_{17} = 3.64$

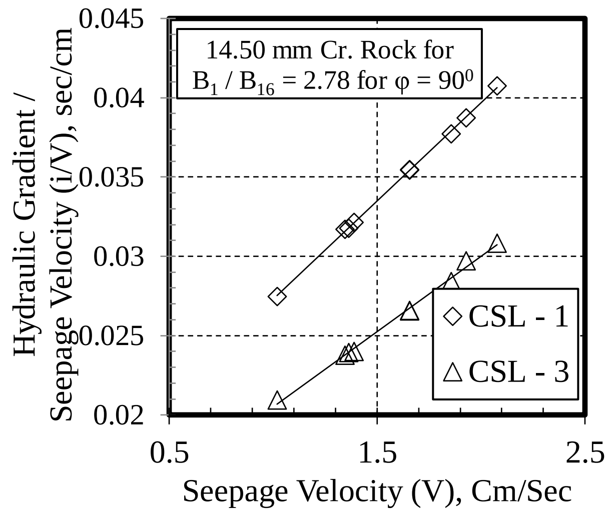

Fig.10.2 i/V vs V for $B_1/B_{16} = 2.78$

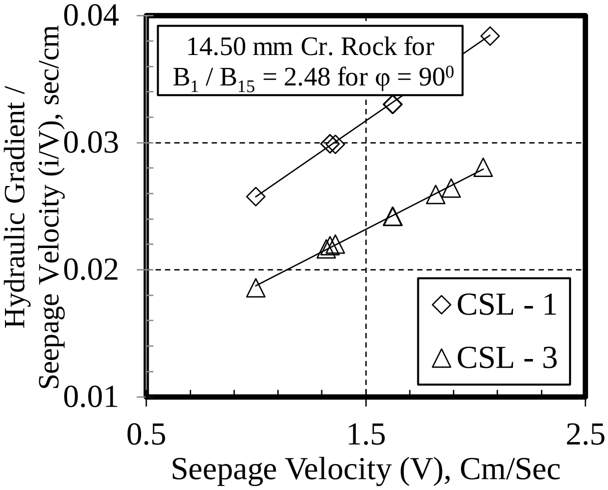

Fig.10.3 i/V vs V for B_1/B_{15} = 2.48

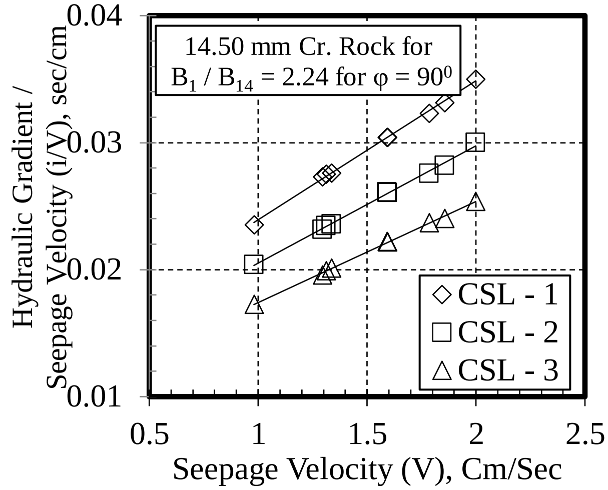

Fig.10.4 i/V vs V for B_1/B_{14} = 2.24

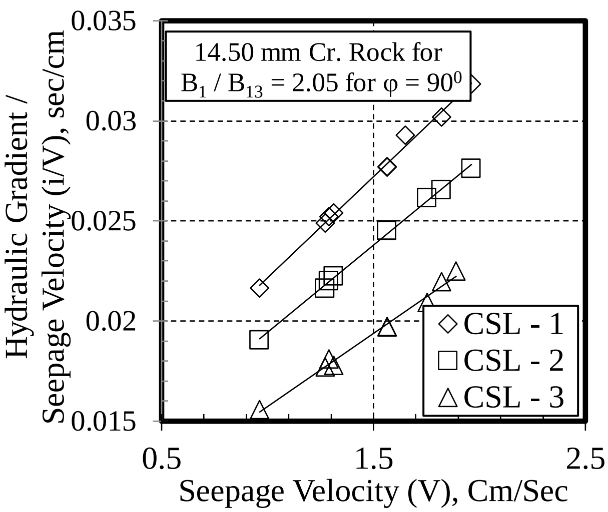

Fig.10.5 i/V vs V for B_1/B_{13} = 2.05

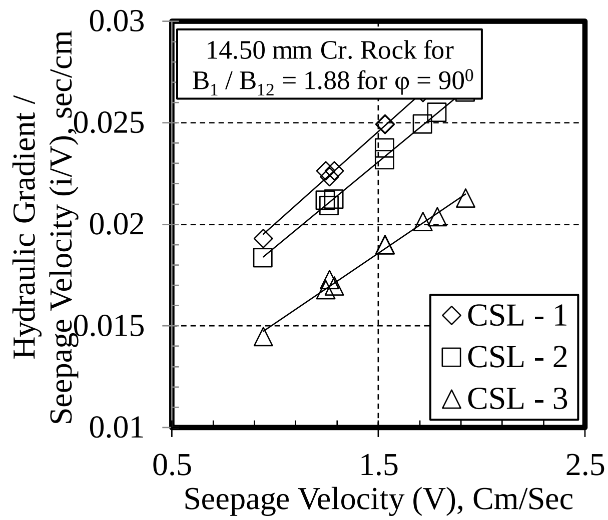

Fig.10.6 i/V vs V for B_1/B_{12} = 1.88

Fig.10 i/V vs V for Different CSL for the same B_1/B_2 Ratios for φ = 90^0 for 14.50 mm Cr. Rock

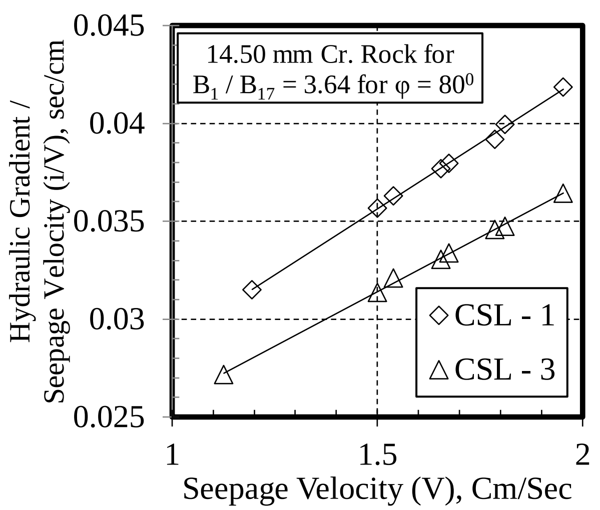

Fig.11.1 i/V vs V for B_1/B_{17} = 3.64

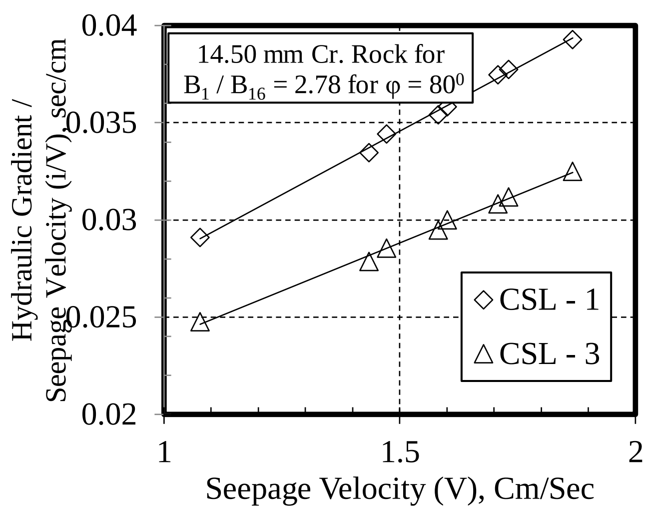

Fig.11.2 i/V vs V for B_1/B_{16} = 2.78

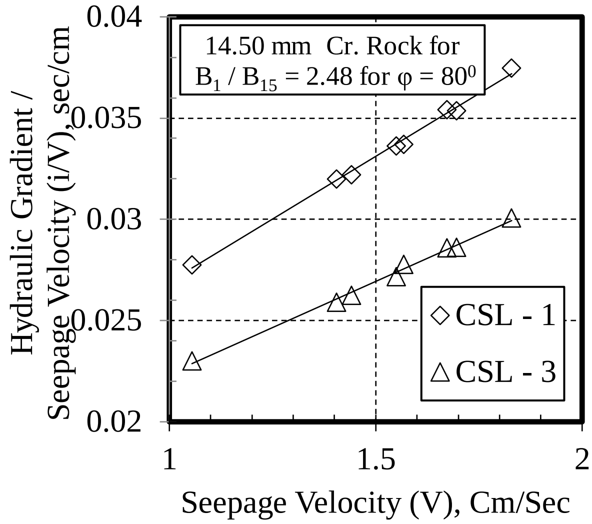

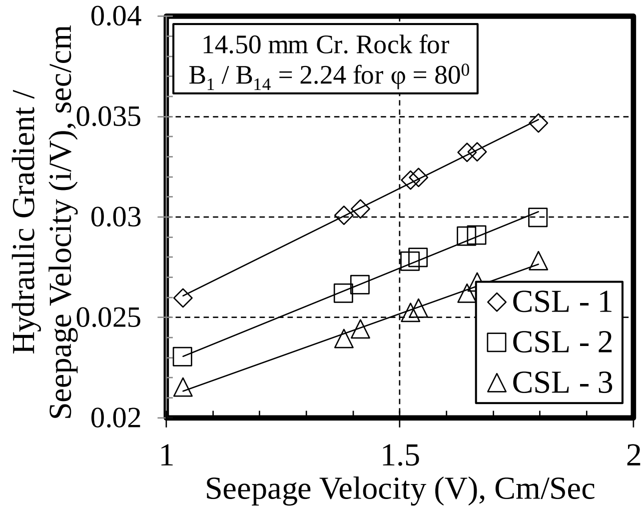

Fig.11.3 i/V vs V for B_1/B_{15} = 2.48 **Fig.11.4 i/V vs V for B_1/B_{14} = 2.24**

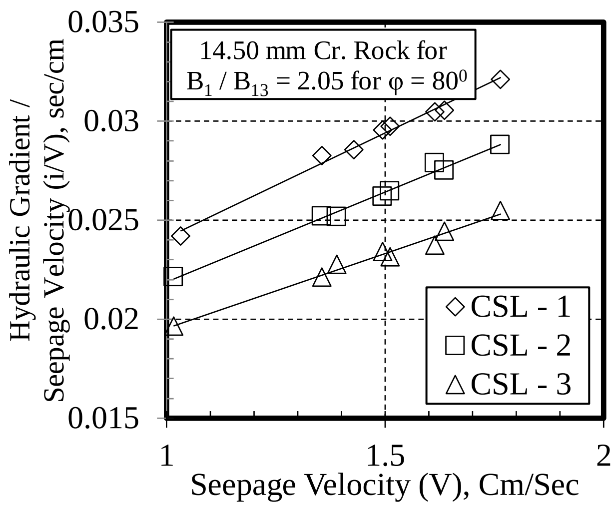

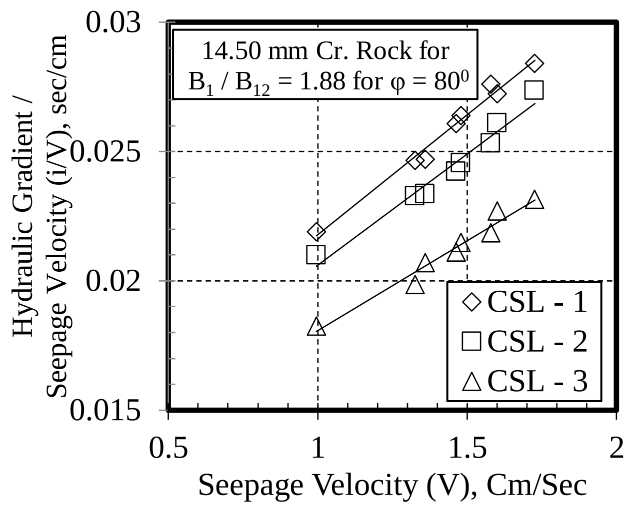

Fig.11.5 i/V vs V for B_1/B_{13} = 2.05 **Fig.11.6 i/V vs V for B_1/B_{12} = 1.88**

Fig.11 i/V vs V for Different CSL for the same B_1/B_2 Ratios for φ = $80^0$for 14.50 mm Cr. Rock

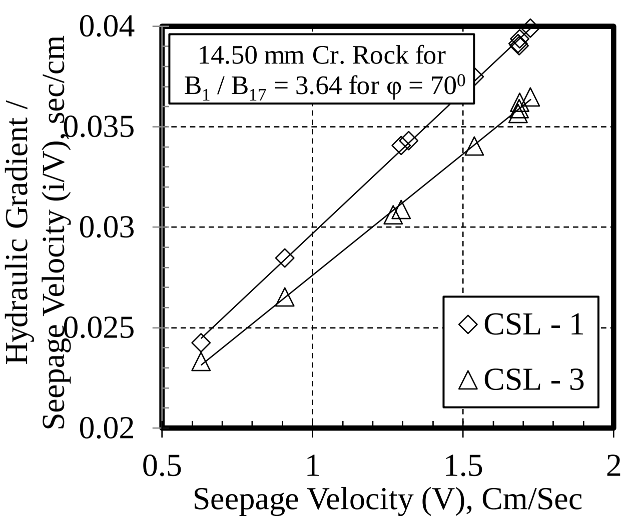

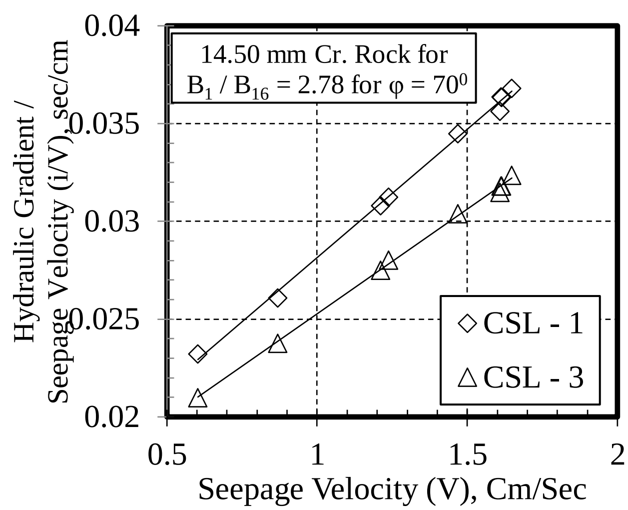

Fig.12.1 i/V vs V for B_1/B_{17} = 3.64

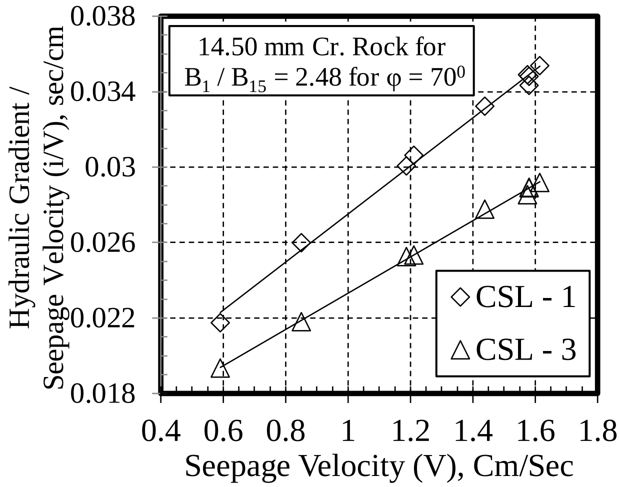

Fig.12.2 i/V vs V for B_1/B_{16} = 2.78

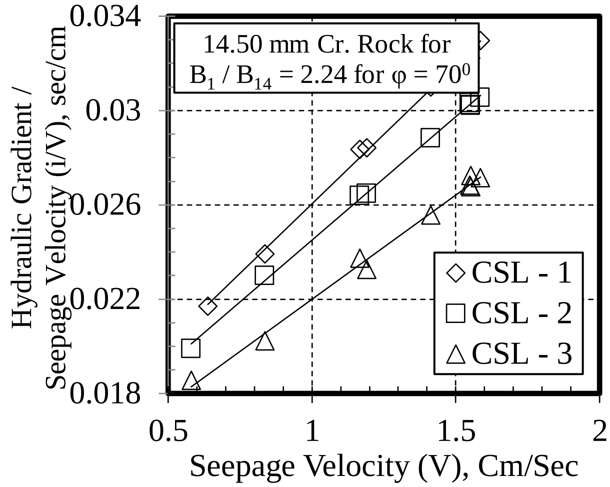

Fig.12.3 i/V vs V for B_1/B_{15} = 2.48

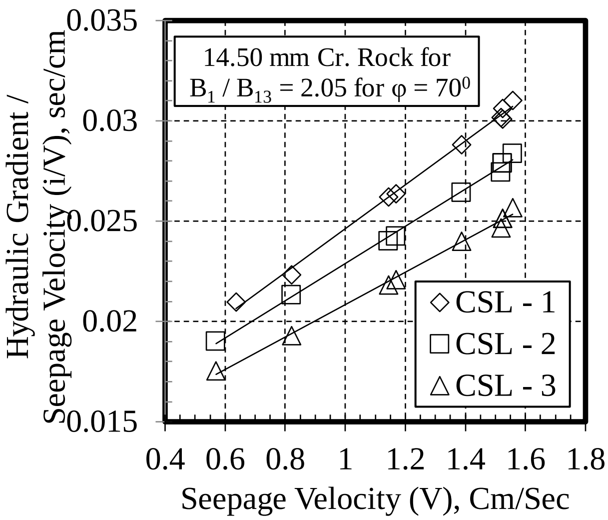

Fig.12.4 i/V vs V for B_1/B_{14} = 2.24

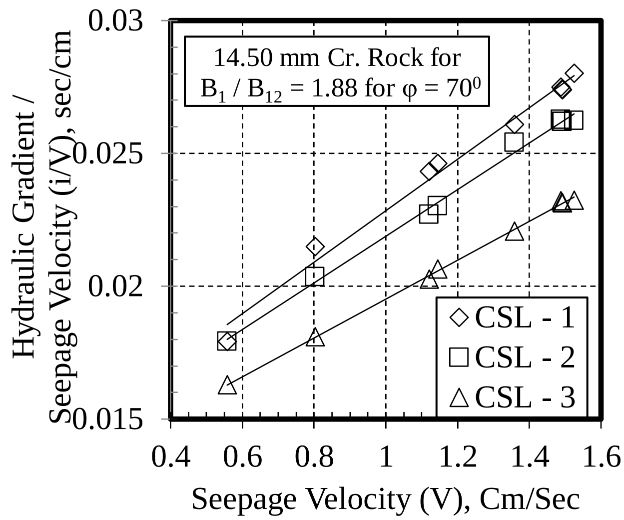

Fig.12.5 i/V vs V for B_1/B_{13} = 2.05

Fig.12.6 i/V vs V for B_1/B_{12} = 1.88

Fig.12 i/V vs V for Different CSL for the same B_1/B_2 Ratios for φ = 70⁰for 14.50 mm Cr. Rock

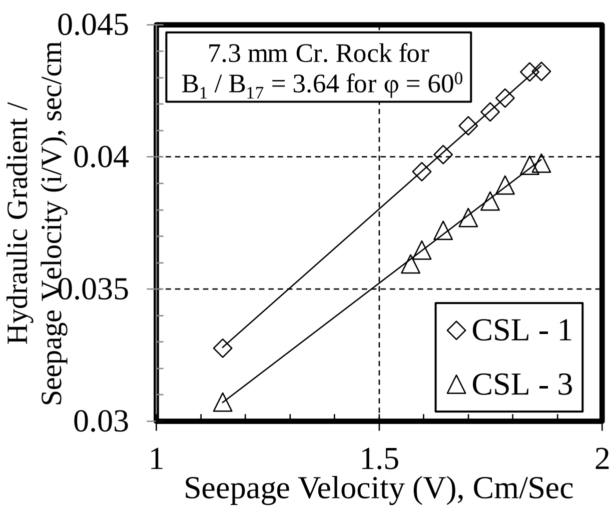

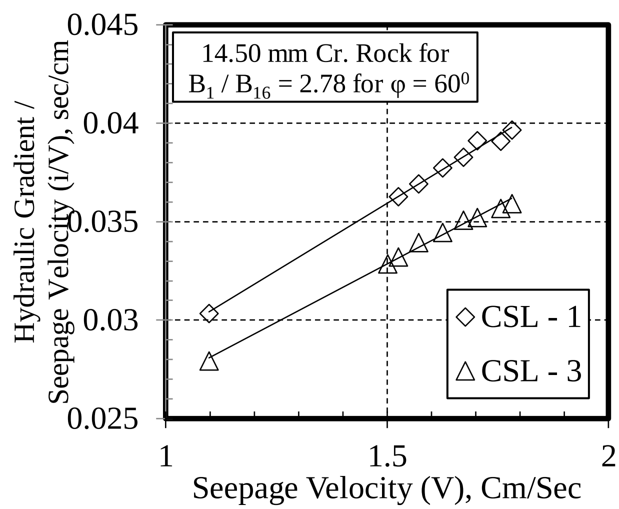

Fig.13.1 i/V vs V for B_1/B_{17} = 3.64

Fig.13.2 i/V vs V for B_1/B_{16} = 2.78

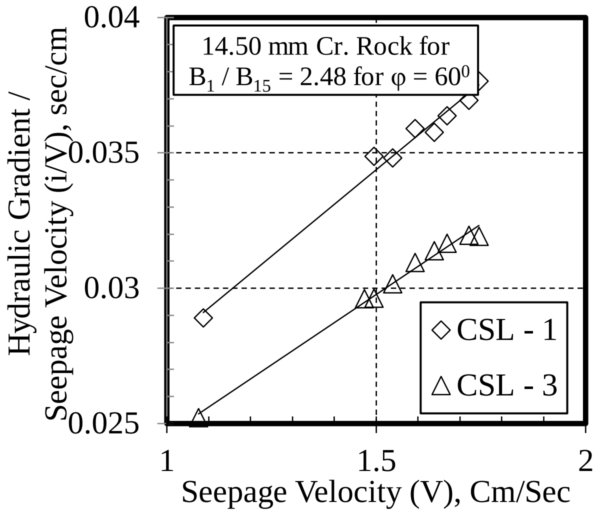

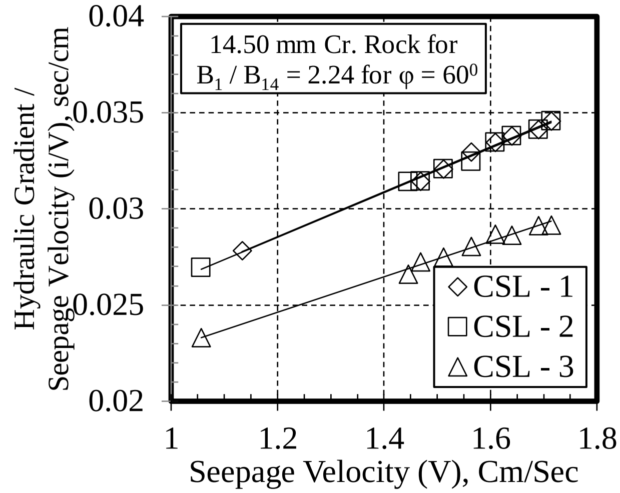

Fig.13.3 i/V vs V for B_1/B_{15} = 2.48

Fig.13.4 i/V vs V for B_1/B_{14} = 2.24

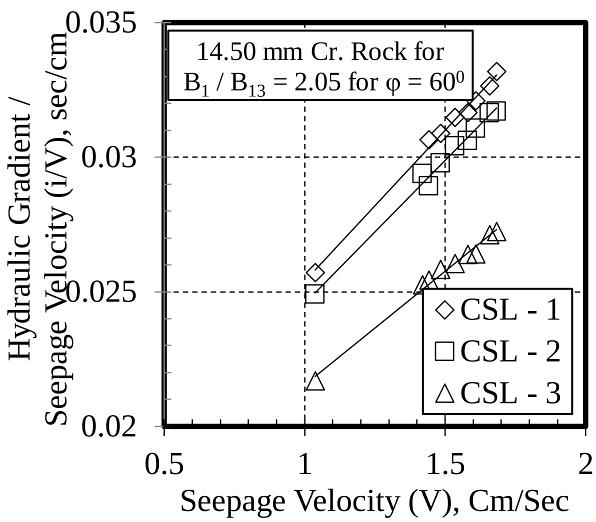

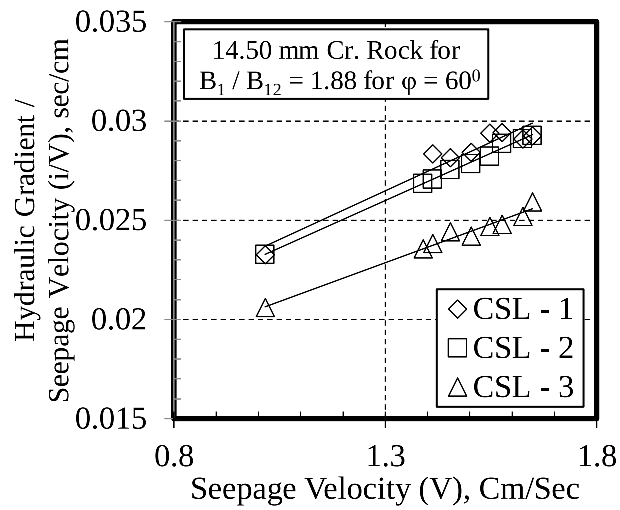

Fig.13.5 i/V vs V for B_1/B_{13} = 2.05

Fig.13.6 i/V vs V for B_1/B_{12} = 1.88

Fig.13 i/V vs V for Different CSL for the same B_1/B_2 Ratios for $\varphi = 60^0$ for 14.50 mm Cr. Rock

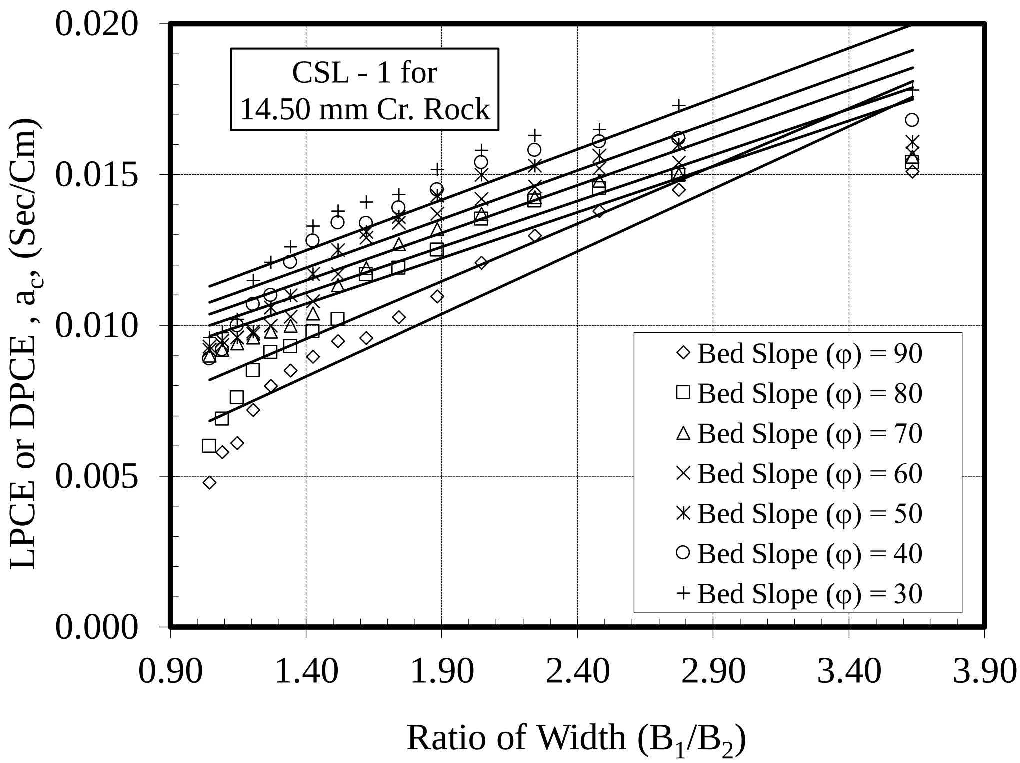

Fig.14.1 Variation of LPCE or DPCE,a_c, with Ratio of Widths, B_1 / B_2

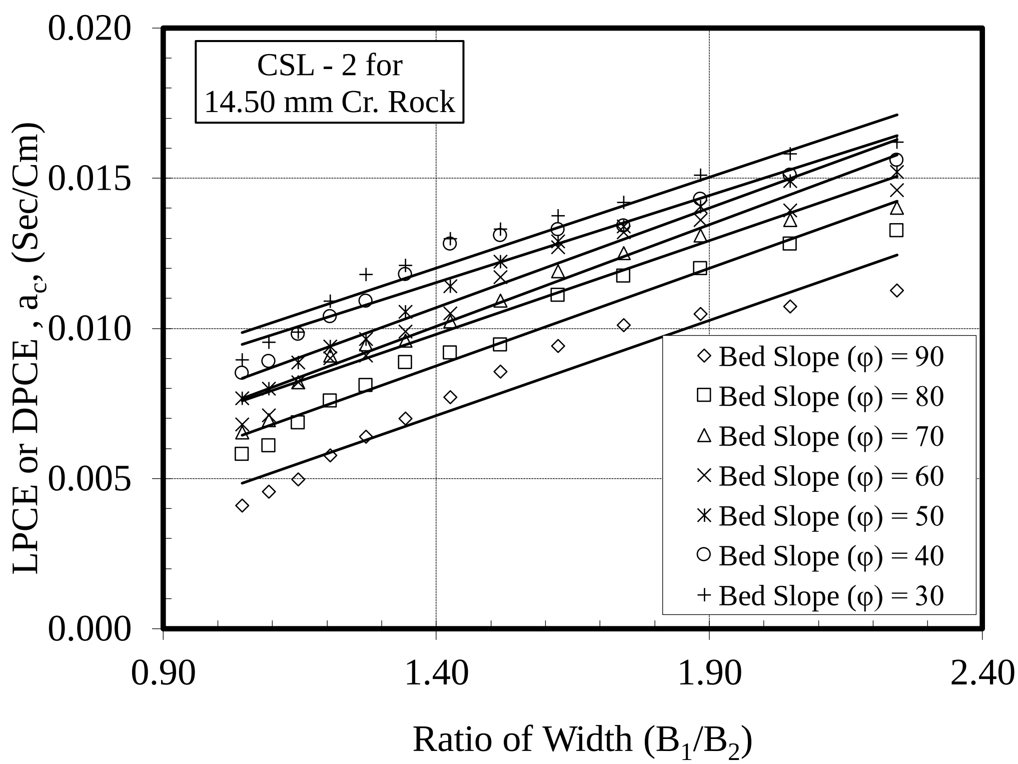

Fig.14.2 Variation of LPCE or DPCE,a_c, with Ratio of Widths, B_1 / B_2

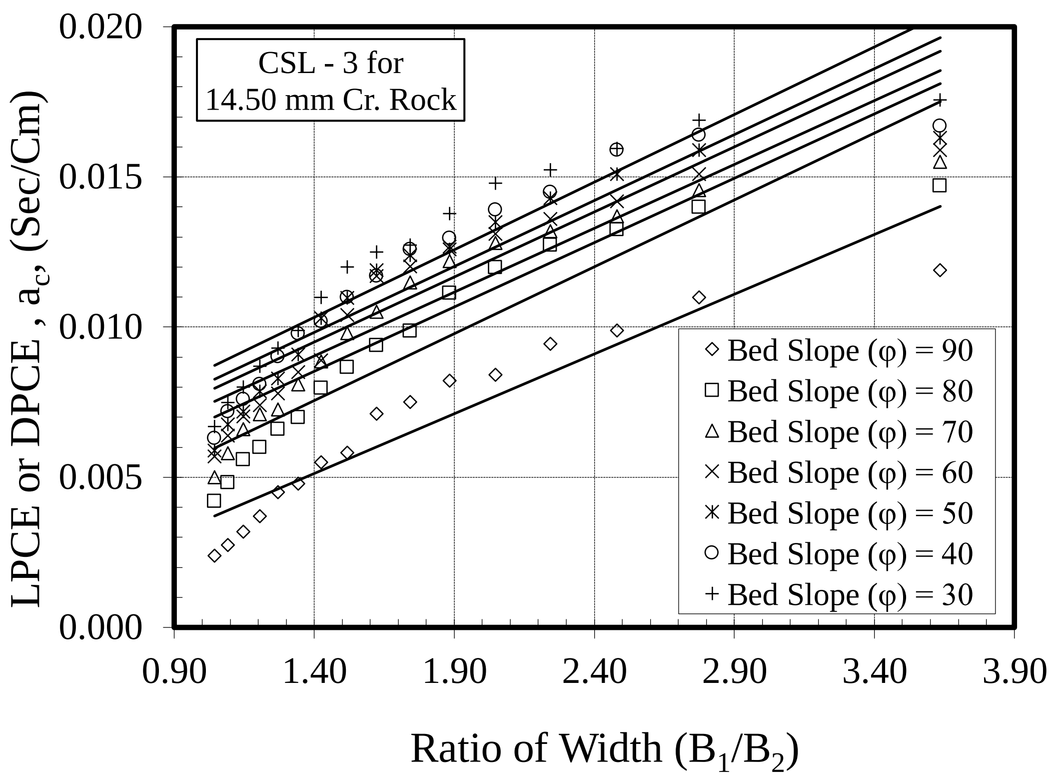

Fig.14.3 Variation of LPCE or DPCE ,a_c, with Ratio of Widths B_1 / B_2

Fig.14 Variation of LPCE or DPCE,a_c, with Ratio of Widths B_1 / B_2 for Different Bed Slopes for 14.50 mm Crushed Rock

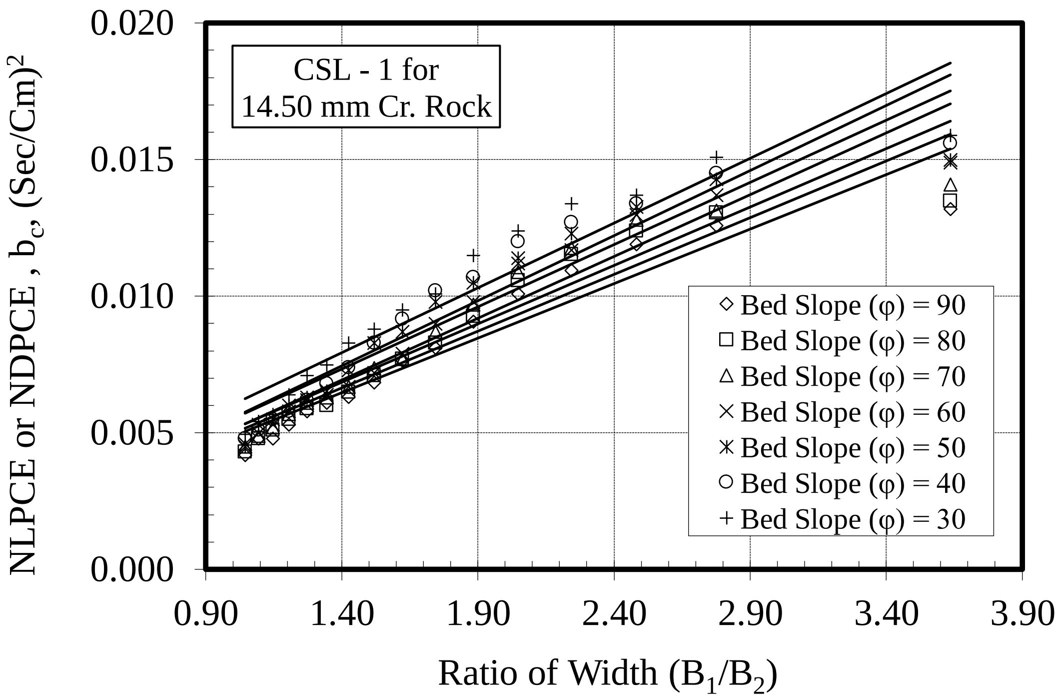

Fig.15.1 Variation of NLPCE or NDPCE , b_c,with Ratio of Widths, B_1 / B_2

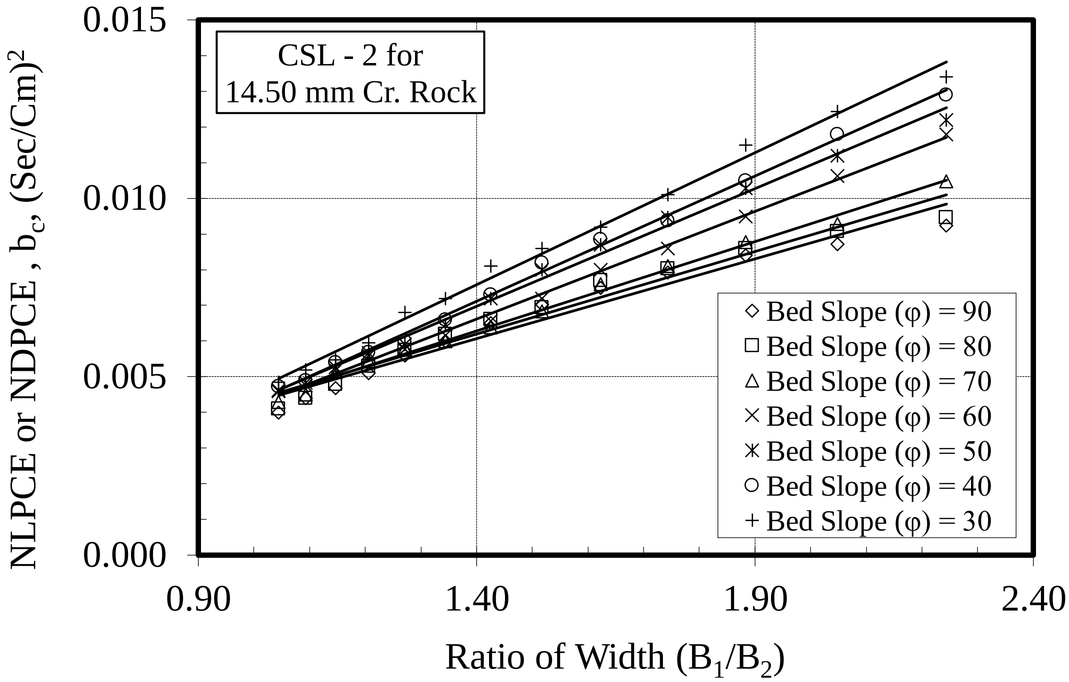

Fig.15.2 Variation of NLPCE or NDPCE , b_c,with Ratio of Widths, B_1 / B_2

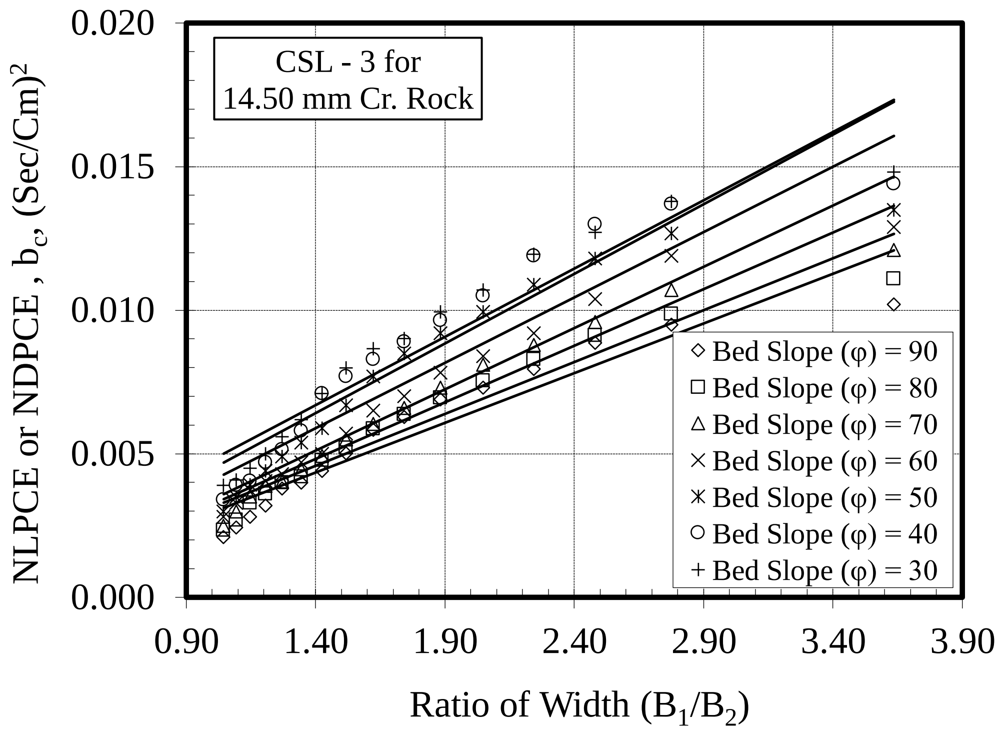

Fig.15.3 Variation of NLPCE or NDPCE , b_c,with Ratio of Widths, B_1 / B_2

Fig.15 Variation of NLPCE or NDPCE , b_c,with Ratio of Widths, B_1 / B_2 for Different Bed Slopes for 14.50 mm Crushed Rock

Table.1 LPCE or DPCE , a_c, and NLPCE or NDPCE, b_c, for different bed slopes (φ) and ratio of widths(B_1/B_2) for 14.50 mm crushed rock for convergent stream line - 1

B_1/B_2	Porosity (N)	CONVERGENT STREAM LINE - 1 FOR 14.50 MM CRUSHED ROCK							
		90		80		70		60	
		a_c	b_c	a_c	b_c	a_c	b_c	a_c	b_c
3.64	0.4168	0.0151	0.0132	0.0154	0.0135	0.0156	0.0141	0.0157	0.0149
2.78	0.4360	0.0145	0.0126	0.0150	0.0131	0.0150	0.0131	0.0154	0.0137
2.48	0.4450	0.0138	0.0119	0.0145	0.0124	0.0148	0.0128	0.0152	0.0130
2.24	0.4531	0.0130	0.0110	0.0141	0.0115	0.0143	0.0118	0.0146	0.0117
2.05	0.4615	0.0121	0.0101	0.0135	0.0106	0.0137	0.0109	0.0142	0.0112
1.88	0.4713	0.0110	0.0091	0.0125	0.0093	0.0132	0.0097	0.0137	0.0098
1.74	0.4817	0.0103	0.0081	0.0119	0.0083	0.0127	0.0087	0.0134	0.0090
1.62	0.4909	0.0096	0.0077	0.0117	0.0077	0.0119	0.0077	0.0129	0.0079
1.52	0.5004	0.0095	0.0068	0.0102	0.0071	0.0113	0.0074	0.0117	0.0072
1.43	0.5076	0.0090	0.0063	0.0098	0.0065	0.0104	0.0067	0.0108	0.0067
1.34	0.5157	0.0085	0.0061	0.0093	0.0060	0.0100	0.0063	0.0103	0.0064
1.27	0.5272	0.0080	0.0058	0.0091	0.0059	0.0098	0.0061	0.0100	0.0062
1.21	0.5396	0.0072	0.0053	0.0085	0.0055	0.0096	0.0057	0.0097	0.0058
1.15	0.5503	0.0061	0.0048	0.0076	0.0051	0.0094	0.0052	0.0096	0.0053
1.09	0.5648	0.0058	0.0048	0.0069	0.0048	0.0092	0.0049	0.0094	0.0050
1.04	0.5890	0.0048	0.0042	0.0060	0.0043	0.0090	0.0045	0.0092	0.0046

Table.2 LPCE or DPCE , a_c, and NLPCE or NDPCE, b_c, for different bed slopes (φ) and ratio of widths (B_1/B_2) for 14.50 mm crushed rock for convergent stream line - 2

B_1/B_2	Porosity (N)	CONVERGENT STREAM LINE - 2 FOR 14.50 MM CRUSHED ROCK							
		90		80		70		60	
		a_c	b_c	a_c	b_c	a_c	b_c	a_c	b_c
2.24	0.4531	0.0113	0.0092	0.0133	0.0095	0.0140	0.0105	0.0146	0.0118
2.05	0.4615	0.0107	0.0087	0.0128	0.0091	0.0136	0.0093	0.0139	0.0106
1.88	0.4713	0.0105	0.0084	0.0120	0.0086	0.0131	0.0088	0.0136	0.0095
1.74	0.4817	0.0101	0.0079	0.0117	0.0080	0.0125	0.0081	0.0132	0.0086
1.62	0.4909	0.0094	0.0075	0.0111	0.0077	0.0119	0.0076	0.0127	0.0080
1.52	0.5004	0.0086	0.0070	0.0095	0.0069	0.0109	0.0068	0.0117	0.0072
1.43	0.5076	0.0077	0.0065	0.0092	0.0066	0.0102	0.0064	0.0105	0.0066
1.34	0.5157	0.0070	0.0060	0.0089	0.0062	0.0096	0.0060	0.0099	0.0062

1.27	0.5272	0.0064	0.0056	0.0081	0.0058	0.0095	0.0058	0.0091	0.0058
1.21	0.5396	0.0058	0.0051	0.0076	0.0053	0.0091	0.0055	0.0090	0.0056
1.15	0.5503	0.0050	0.0047	0.0069	0.0048	0.0082	0.0051	0.0082	0.0052
1.09	0.5648	0.0046	0.0044	0.0061	0.0044	0.0069	0.0045	0.0071	0.0048
1.04	0.5890	0.0041	0.0040	0.0058	0.0041	0.0065	0.0043	0.0068	0.0046

Table.3 LPCE or DPCE , a_c, and NLPCE or NDPCE, b_c, for different bed slopes (φ) and ratio of widths (B_1/B_2) for 14.50 mm crushed rock for convergent stream line - 3

B_1/B_2	**Porosity (N)**	**CONVERGENT STREAM LINE - 3 FOR 14.50 MM CRUSHED ROCK**							
		90		**80**		**70**		**60**	
		a_c	**b_c**	**a_c**	**b_c**	**a_c**	**b_c**	**a_c**	**b_c**
3.64	0.4168	0.0119	0.0102	0.0147	0.0111	0.0155	0.0121	0.0159	0.0129
2.78	0.4360	0.0110	0.0095	0.0140	0.0099	0.01456	0.01071	0.0151	0.0119
2.48	0.4450	0.0099	0.0089	0.0133	0.0091	0.0137	0.0096	0.0142	0.0104
2.24	0.4531	0.0094	0.0080	0.0127	0.0083	0.0132	0.0088	0.0136	0.0092
2.05	0.4615	0.0084	0.0073	0.0120	0.0076	0.0128	0.0081	0.0131	0.0084
1.88	0.4713	0.0082	0.0069	0.0111	0.0070	0.0122	0.0073	0.01269	0.00782
1.74	0.4817	0.0075	0.0063	0.0099	0.0064	0.0115	0.0066	0.01203	0.007
1.62	0.4909	0.0071	0.0058	0.0094	0.0059	0.01052	0.00605	0.0117	0.0065
1.52	0.5004	0.0058	0.0050	0.0087	0.0052	0.0098	0.0055	0.0104	0.0057
1.43	0.5076	0.0055	0.0044	0.0080	0.0048	0.00886	0.00493	0.0089	0.005
1.34	0.5157	0.0048	0.0040	0.0070	0.0042	0.0081	0.00446	0.0085	0.0047
1.27	0.5272	0.0045	0.0038	0.0066	0.0040	0.00726	0.00403	0.0078	0.0043
1.21	0.5396	0.0037	0.0032	0.0060	0.0036	0.0071	0.00388	0.0074	0.00405
1.15	0.5503	0.0032	0.0028	0.0056	0.0033	0.0066	0.00352	0.00704	0.00374
1.09	0.5648	0.0028	0.0024	0.0048	0.0027	0.0058	0.003	0.0064	0.0033
1.04	0.5890	0.0024	0.0021	0.0042	0.0024	0.005	0.0025	0.0057	0.0028